

Runge–Kutta generalized Convolution Quadrature for sectorial problems

J. Guo ^{*} M. Lopez-Fernandez[†]

June 27, 2025

Abstract

We study the application of the generalized convolution quadrature (gCQ) based on Runge–Kutta methods to approximate the solution of an important class of sectorial problems. The gCQ generalizes Lubich’s original convolution quadrature (CQ) to variable steps. High-order versions of the gCQ have been developed in the last decade, relying on certain Runge–Kutta methods. The Runge–Kutta based gCQ has been studied so far in a rather general setting, which includes applications to boundary integral formulations of wave problems. The available stability and convergence results for these new methods are suboptimal compared to those known for the uniform-step CQ, both in terms of convergence order and regularity requirements of the data. Here we focus on a special class of sectorial problems and prove that in these important applications it is possible to achieve the same order of convergence as for the original CQ, under the same regularity hypotheses on the data, and for very general time meshes. In the particular case of data with some known algebraic type of singularity, we also show how to choose an optimally graded time mesh to achieve convergence with maximal order, overcoming the well-known order reduction of the original CQ in these situations. An important advantage of the gCQ method is that it allows for a fast and memory-efficient implementation. We describe how the fast and oblivious Runge–Kutta based gCQ can be implemented and illustrate our theoretical results with several numerical experiments. The codes implementing the examples in this article are available in [13].

Keywords: generalized convolution quadrature, sectorial problems, variable steps, graded meshes, fractional differential equations, equations with memory.

AMS subject classifications: 65R20, 65L06, 65M15, 26A33, 35R11.

1 Introduction

In this work, we consider the high-order numerical approximation of Volterra-type convolution operators of the abstract form

$$u(t) = \int_0^t k(t-s)f(s) ds, \quad t > 0, \quad (1)$$

on general non-uniform temporal meshes

$$\Delta := \{0 = t_0 < t_1 < \cdots < t_N = T\}, \quad (2)$$

^{*}Department of Mathematics, University of Macau, Macao SAR, China. Email: jingguo@um.edu.mo

[†]Department of Mathematical Analysis, Statistics and O.R., and Applied Mathematics. Faculty of Sciences. University of Malaga. Bulevar Louis Pasteur, 31 29010 Malaga, Spain. Email: maria.lopezf@uma.es

with step sizes defined as

$$\tau_n := t_n - t_{n-1}, \quad n = 1, \dots, N.$$

The maximum and minimum step sizes are denoted by

$$\tau_{\max} := \max_{1 \leq j \leq N} \tau_j, \quad \tau_{\min} := \min_{1 \leq j \leq N} \tau_j. \quad (3)$$

The numerical discretization of (1) has been extensively studied due to its appearance in a wide range of models, including fractional differential equations [4, 18, 26, 32, 31], viscoelasticity [12] and time-domain boundary integral equations [7, 27, 30]. The convolution kernel $k(t)$ can take various forms depending on the problem setting. Typical examples include scalar-valued kernels like $k(t) = t^\alpha$ with $\alpha > -1$, which arise in fractional integral operators [4, 33, 24]; operator-valued kernels such as $k(t) = e^{\mathcal{A}t}$, representing semigroups generated by linear operators [20, 10]; and Green's functions in boundary integral equations [5, 34], including distributional kernels such as the Dirac delta that appears in wave propagation problems [9, Chapter 2].

Let $K(z)$ denote the Laplace transform of $k(t)$. We assume that K acts as a bounded linear operator between normed vector spaces \mathcal{X} and \mathcal{Y} , with norm

$$\|K(z)\| := \sup_{u \in \mathcal{X}, \|u\|_{\mathcal{X}}=1} \|K(z)u\|_{\mathcal{Y}}.$$

The Laplace transform $K(\cdot)$, which is referred to as the *transfer operator* in many applications, plays a fundamental role in Convolution Quadrature (CQ) methods, introduced in Lubich's pioneering work [25, 26]. In this work, we focus on a special class of sectorial problems, characterized by the following conditions on K :

Assumption 1. *The transfer operator K satisfies:*

1. *K is holomorphic in the sector $|\arg(z)| < \pi$.*
2. *There exist constants $M > 0$ and $\alpha \in (0, 1)$ such that*

$$\|K(z)\|_{\mathcal{X} \rightarrow \mathcal{Y}} \leq M|z|^{-\alpha}, \quad |\arg(z)| < \pi. \quad (4)$$

3. *K is continuous in the closed upper half-plane $\operatorname{Im} z \geq 0$, except possibly at $z = 0$, and similarly on the lower edge of the branch cut.*

When unambiguous, norm subscripts are omitted. The conditions on $K(z)$ cover a large and important range of examples, such as $K(z) = z^{-\alpha}$, which corresponds to fractional integrals [4, 18, 24, 32]; $K(z) = (z^\alpha + r)^{-1}$ with $r > 0$, which is the Laplace transform of kernels usually used in damped wave models, see for instance [1]; also $K(z) = (z^\alpha I + \mathcal{A})^{-1}$, where \mathcal{A} is a symmetric positive definite operator or matrix [14, 16, 17].

Under Assumption 1, the convolution kernel k admits a real integral representation, cf. [4, 14]:

$$k(t) = \int_0^\infty e^{-xt} G(x) dx, \quad G(x) := \frac{K(xe^{-i\pi}) - K(xe^{i\pi})}{2\pi i}, \quad (5)$$

with the operator G satisfying the bound

$$\|G(x)\| \leq \frac{M}{\pi} x^{-\alpha}, \quad x > 0, \quad 0 < \alpha < 1. \quad (6)$$

For the particular example of the fractional integral, with $k(t) = t^{\alpha-1}/\Gamma(\alpha)$, the corresponding function $G(x)$ is given by

$$G(x) = \frac{\sin(\pi\alpha)}{\pi} x^{-\alpha}. \quad (7)$$

For $K(z) = (z^\alpha I + \mathcal{A})^{-1}$, explicit formulas for G are derived in [14, Section 4]. Other examples are considered in detail in Section 6.

The representation in (5) has been successfully employed in [4] for the efficient numerical solution of subdiffusion equations on uniform temporal grids, allowing for a special fast and oblivious quadrature which significantly improves the computational efficiency, the memory requirements and the coding. In [8], the Euler based gCQ weights for the fractional derivative are derived using (7), and *a posteriori* error estimates for the application of this method to the subdiffusion equation are established. The study in [14] is also based on (5), where under Assumption 1, optimal *a priori* error bounds are proven for the Euler based gCQ method, together with a generalization of the fast and oblivious algorithm in [4] to the case of general nonuniform meshes. So far all available studies based on (5) for the gCQ are limited to the first order version of it. High order versions of the gCQ based on Runge–Kutta methods have been proposed and analyzed in [23] for more general problems than the ones considered in the present manuscript, for which high order but non optimal error estimates are proven, under very strong regularity assumptions on the data f .

Original CQ methods, defined on uniform time meshes, require quite some regularity of the input data $f(t)$ in order to achieve their maximal order. In particular, the extension of f to $t < 0$ by 0 is typically required to be several times differentiable, which leads to the request that a certain number of the moments of f at $t = 0$ vanish [29, 6]. In many practical applications this is not the case and a well known order reduction takes place [25], even if correction terms can be added to improve the performance at times away from 0, see for instance [8, 10, 16, 28]. Moreover, singularities of the data f at other time points can not be properly resolved by the original CQ formulas. This limitations have motivated the development and analysis of the so-called generalized Convolution Quadrature (gCQ) methods [2, 21, 22, 23, 14]. In particular, under Assumption 1, a sharp error analysis is performed in [14], for data f satisfying the minimal regularity requirement

$$f(t) = t^\beta g(t), \quad \beta > -1, \quad (8)$$

where g is smooth. In this work, the study in [14] is generalized to high-order gCQ based on Runge–Kutta methods. We actually improve further the regularity requirements on the data f in [14] by using distributional derivatives rather than the mean value theorem in the estimation of the local error reminders, see Remark 21. In this way, for problems satisfying Assumption 1, we manage to achieve full order of convergence for the Runge–Kutta gCQ under the very same assumptions as the original Lubich’s CQ with uniform step size, see [29].

In what follows we consider s -stage Runge–Kutta schemes with coefficient matrix \mathbf{A} , weights \mathbf{b} , and abscissas \mathbf{c} , satisfying the following conditions.

Assumption 2. *The Runge–Kutta method is A-stable, that is,*

$$|R(z)| \leq 1 \quad \text{for } \operatorname{Re} z \leq 0, \quad (9)$$

with classical order $p \geq 1$, stage order $q \leq p$, and is stiffly accurate, meaning

$$\mathbf{b} = \mathbf{A}^\top \mathbf{e}_s, \quad \text{with } \mathbf{e}_s = (0, \dots, 0, 1)^\top \in \mathbb{R}^s. \quad (10)$$

Notice that (5) yields the alternative formulation of (1):

$$u(t) = \int_0^\infty G(x)y(x, t) dx,$$

where $y(x, t)$ satisfies

$$\partial_t y(x, t) = -xy(x, t) + f(t), \quad y(x, 0) = 0. \quad (11)$$

The gCQ approximation u_n to $u(t)$ at t_n , for $1 \leq n \leq N$, is obtained by applying the s -stage Runge–Kutta method to approximate $y(x, t_n)$, this is

$$u_n = \int_0^\infty G(x) y_n(x) dx,$$

with $y_n(x) \approx y(x, t_n)$. This definition of u_n is equivalent to the definition in [23] for general problems (1), where a complex contour integral representation is needed for both $u(t)$ and its numerical approximation. In the general setting, the following convergence result was established in [23]:

Theorem 3 (Theorem 16 in [23]). *Assume that the Runge–Kutta method satisfies Assumption 2, $f \in C^{p+2}([0, T])$ and $f^{(\ell)}(0) = 0$ for all $0 \leq \ell \leq q$. Then, it holds*

$$\|u(t_n) - u_n\|_{\mathcal{Y}} \leq C e^{\sigma T} \tau_{\max}^q \|f\|_{C^{p+2}([0, T], \mathcal{X})}, \quad n \geq 1.$$

Here we analyze the error of the Runge–Kutta based gCQ method applied to (1), with $f(t)$ like in (8). More precisely, we assume that f admits the fractional power expansion

$$f(t) = \sum_{\ell=0}^m \frac{f^{(\ell+\beta)}(0)}{\Gamma(\ell+\beta+1)} t^{\ell+\beta} + \frac{1}{\Gamma(m+\beta+1)} \left(t^{m+\beta} * f^{(m+\beta+1)} \right) (t), \quad (12)$$

with the Riemann–Liouville derivative of order $\mu > 0$ defined as

$$f^{(\mu)}(t) = \frac{d^\nu}{dt^\nu} \left(\int_0^t \frac{(t-s)^{\nu-\mu-1}}{\Gamma(\nu-\mu)} f(s) ds \right),$$

with $\nu := \lceil \mu \rceil$. The following Theorem is the main result of this paper and establishes the convergence error bounds of the Runge–Kutta based gCQ for problems satisfying Assumption 1.

Theorem 4. *For $f(t)$ admitting the expansion (12) with $\beta > -1$ and $m = \lceil p - \beta - 1 \rceil$, under Assumptions 1 and 2, the following error estimates hold true.*

- (i) *If $f^{(\ell+\beta)}(0) = 0$ for all $\ell = 0, 1, \dots, \lceil p - \alpha - \beta - 1 \rceil$, then on the general mesh (2), the error satisfies*

$$\|u(t_n) - u_n\|_{\mathcal{Y}} \leq CM |\log(\tau_{\min})| \tau_{\max}^{\min\{p, q+1+\alpha\}} \left\| f^{(m+\beta+1)} \right\|_{C^0([0, t_n], \mathcal{X})}, \quad n \geq 1.$$

In particular, for the general mesh (2), the full convergence order $\min\{p, q+1+\alpha\}$ is achieved when $f \in C^p([0, T]; \mathcal{X})$ and satisfies the vanishing moment conditions $f^{(\ell)}(0) = 0$ for all $\ell = 0, 1, \dots, p-1$, which corresponds to the case $\beta = 0$.

- (ii) *If the mesh (2) is quasi-uniform, i.e.,*

$$c_\Delta := \frac{1}{2} \max_{2 \leq i \leq N} \left(\frac{\tau_i}{\tau_{i-1}} + \frac{\tau_{i-1}}{\tau_i} \right) \quad (13)$$

is a bounded constant, and

$$f^{(\ell+\beta)}(0) = 0 \quad \text{for all } \ell = 0, 1, \dots, \min\{\lceil p - \alpha - \beta - 1 \rceil, \lceil q - \beta \rceil\},$$

then for all $n \geq 1$, the error satisfies

$$\|u(t_n) - u_n\|_{\mathcal{Y}} \leq CM c_\Delta^{\max\{0, p-q-\alpha\}} |\log(\tau_{\min})| \tau_{\max}^{\min\{p, q+1+\alpha\}} \left\| f^{(m+\beta+1)} \right\|_{C^0([0, t_n], \mathcal{X})}.$$

Here, C is a positive constant independent of the mesh.

For graded meshes, which are quasi-uniform, the error can be estimated more precisely, without assuming any vanishing moments of the data f at the origin.

Theorem 5. *Suppose $f(t)$ admits an expansion of the form (12) with $\beta > -1$ and $m = \lceil p - \beta - 1 \rceil$. Under Assumptions 1 and 2, the error of the Runge–Kutta based gCQ method for (1) on the graded mesh*

$$t_n = (n\tau)^\gamma, \quad \tau = \frac{T^{1/\gamma}}{N}, \quad n = 1, \dots, N, \quad \gamma \geq 1, \quad (14)$$

satisfies

$$\begin{aligned} \|u(t_n) - u_n\|_Y &\leq CM \sum_{\ell=0}^m \log(N) N^{-\min\{\gamma(\alpha+\ell+\beta), p, q+1+\alpha\}} \|f^{(\ell+\beta)}(0)\|_{\mathcal{X}} \\ &\quad + CM \log(N) N^{-\min\{p, q+1+\alpha\}} \left\| f^{(m+1+\beta)} \right\|_{C^0([0, t_n], \mathcal{X})}, \end{aligned}$$

where C denotes a positive constant independent of the mesh.

The paper is organized as follows. Section 2 presents the framework of the Runge–Kutta based gCQ scheme. Section 3 establishes the stability analysis, while Section 4 derives error estimates for general and quasi-uniform meshes, along with a grading strategy for graded meshes. Implementation details, including a fast algorithm for computing convolution integrals and its application to subdiffusion equations, are discussed in Section 5. The numerical experiments in Section 6 evaluate the performance of the proposed algorithm for convolution integrals, subdiffusion equations, and nonlinear wave equations with damping terms of the form (1). In all cases, the Runge–Kutta based gCQ scheme achieves significantly reduced maximum absolute errors compared to the uniform step size approximation provided by original Lubich’s CQ, cf. [16] for the subdiffusion equation and [1] for the damped Westervelt equation. In particular, for the nonlinear Westervelt equation considered in [3], employing the two-stage Radau–IIA gCQ method on a suitable graded mesh increases the convergence order from $1 + \alpha$ to 3. Also, the achieved errors are perfectly consistent with our theoretical results and much better than predicted by the available theory up to date in [23].

2 Runge–Kutta based generalized convolution quadrature

In this section, the formulation of Runge–Kutta based gCQ on the real axis is developed. The s -stage Runge–Kutta method, applied to (11) on the time mesh (2), defines the stage vectors $\mathbf{Y}_n(x)$ and solutions $y_n(x)$ via

$$\mathbf{Y}_n(x) = y_{n-1}(x)\mathbb{1} + \tau_n \mathbf{A}(-x\mathbf{Y}_n(x) + \mathbf{f}_n), \quad n \geq 1, \quad (15a)$$

$$y_n(x) = y_{n-1}(x) + \tau_n \mathbf{b}^\top (-x\mathbf{Y}_n(x) + \mathbf{f}_n), \quad n \geq 1, \quad (15b)$$

where $\mathbf{Y}_n = (Y_{ni})_{i=1}^s$, $\mathbb{1} = (1)_{i=1}^s$, $\mathbf{f}_n = (f(t_{n-1} + c_i \tau_n))_{i=1}^s$. Rewriting (15) as recurrences for \mathbf{Y}_n and y_n yields

$$\mathbf{Y}_n(x) = \mathbf{R}(-\tau_n x) \mathbf{e}_s^\top \mathbf{Y}_{n-1}(x) + \tau_n \mathbf{A}(\mathbf{I} + \tau_n x \mathbf{A})^{-1} \mathbf{f}_n, \quad n \geq 1,$$

and

$$y_n(x) = R(-\tau_n x) y_{n-1}(x) + \tau_n \mathbf{b}^\top (\mathbf{I} + \tau_n x \mathbf{A})^{-1} \mathbf{f}_n, \quad n \geq 1. \quad (16)$$

Here,

$$\mathbf{R}(z) = (\mathbf{I} - z\mathbf{A})^{-1}\mathbb{1}, \quad (17)$$

and the stability function is

$$R(z) = \mathbf{e}_s^\top \mathbf{R}(z) = 1 + z\mathbf{b}^\top (\mathbf{I} - z\mathbf{A})^{-1}\mathbb{1}. \quad (18)$$

Solving the recursion relations yields

$$\mathbf{Y}_n(x) = \sum_{j=1}^n \left(\prod_{l=j+1}^n \mathbf{R}(-\tau_l x) \mathbf{e}_s^\top \right) \tau_j \mathbf{A} (\mathbf{I} + \tau_j x \mathbf{A})^{-1} \mathbf{f}_j, \quad n \geq 1, \quad (19)$$

$$y_n(x) = \sum_{j=1}^n \left(\prod_{l=j+1}^n R(-\tau_l x) \right) \tau_j \mathbf{b}^\top (\mathbf{I} + \tau_j x \mathbf{A})^{-1} \mathbf{f}_j, \quad n \geq 1, \quad (20)$$

where

$$\prod_{l=j+1}^n \mathbf{R}(-\tau_l x) \mathbf{e}_s^\top = \mathbf{R}(-\tau_n x) \mathbf{e}_s^\top \cdots \mathbf{R}(-\tau_{j+1} x) \mathbf{e}_s^\top,$$

with initial conditions $\mathbf{Y}_0(x) = \mathbf{0}$ and $y_0(x) = 0$. The Runge–Kutta based gCQ approximation to (1) is then defined as follows:

Definition 6. For $n \geq 1$, the Runge–Kutta based gCQ approximation to (1) on the time mesh (2) is defined by

$$u_n = \int_0^\infty G(x) y_n(x) dx, \quad (21)$$

with $y_n(x)$ given in (20).

Let $\mathbf{U}(t_n) := (u(t_{n-1} + c_i \tau_n))_{i=1}^s$. The Runge–Kutta based gCQ approximation to $\mathbf{U}(t_n)$ is given by

$$\mathbf{U}_n := \int_0^\infty G(x) \mathbf{Y}_n(x) dx, \quad 1 \leq n \leq N, \quad (22)$$

where $\mathbf{Y}_n(x)$ is given in (19). Define the gCQ weights

$$\mathbf{W}_{n,j} := \tau_j \int_0^\infty G(x) \left(\prod_{l=j+1}^n \left(\mathbf{R}(-\tau_l x) \mathbf{e}_s^\top \right) \right) (\mathbf{A} (\mathbf{I} + \tau_j x \mathbf{A})^{-1}) dx, \quad (23)$$

then the gCQ scheme for the internal stages can be expressed as

$$\mathbf{U}_n = \sum_{j=1}^n \mathbf{W}_{n,j} \mathbf{f}_j, \quad 1 \leq n \leq N, \quad (24)$$

where u_n is the last component of \mathbf{U}_n . The weights (23) also admit an alternative representation as contour integrals [23]:

$$\mathbf{W}_{n,j} = \frac{\tau_j}{2\pi i} \int_\Gamma K(z) \left(\prod_{l=j+1}^n \left(\mathbf{R}(\tau_l z) \mathbf{e}_s^\top \right) \right) (\mathbf{A} (\mathbf{I} - \tau_j z \mathbf{A})^{-1}) dz. \quad (25)$$

3 Stability

The Runge–Kutta method satisfying Assumption 2 has the following properties:

1. By (9), the eigenvalues of \mathbf{A}^{-1} lie in the region $\operatorname{Re} z > 0$, implying that \mathbf{A} is invertible and its eigenvalues are also in $\operatorname{Re} z > 0$.
2. From [15, Theorem 4.12], the matrix \mathbf{A} has s distinct eigenvalues. Hence, \mathbf{A} is diagonalizable, i.e., there exists an invertible matrix $\mathbf{P} = (p_{ij})_{i,j=1}^s$ consisting of all eigenvectors of \mathbf{A} such that

$$\mathbf{A} = \mathbf{P}^{-1} \Lambda \mathbf{P}, \quad (26)$$

where

$$\Lambda = \operatorname{diag}([\lambda_1, \dots, \lambda_s]), \quad \lambda_{\min} = \min_{1 \leq i \leq s} \operatorname{Re} \lambda_i, \quad (27)$$

and $\mathbf{A}\mathbf{P}(:, i) = \lambda_i \mathbf{P}(:, i)$ for $1 \leq i \leq s$.

3. The function $R(z)$ satisfies

$$R(\infty) = 0, \quad R(0) = R'(0) = 1. \quad (28)$$

Lemma 7. [20, 19] Assume that the s -stage Runge–Kutta method satisfies Assumption 2, then there exists a constant $\hat{b} > 0$ such that

$$|R(-x)| \leq \frac{1}{1 + \hat{b}x}, \quad \text{for all } x > 0. \quad (29)$$

Lemma 8. Under Assumptions 1 and 2, the gCQ weights given in (23) satisfy

$$\|\mathbf{W}_{n,j}\| \leq CM\tau_j(t_n - t_{j-1})^{\alpha-1}, \quad n \geq j \geq 1. \quad (30)$$

Proof. Applying the bound (6) to (23) yields

$$\|\mathbf{W}_{n,j}\| \leq \frac{M\tau_j}{\pi} \int_0^\infty x^{-\alpha} \|\mathbf{A}(\mathbf{I} + \tau_j x \mathbf{A})^{-1}\| \left\| \mathbf{R}(-\tau_n x) \mathbf{e}_s^\top \right\| \left| \prod_{l=j+1}^{n-1} R(-\tau_l x) \right| dx,$$

where $\mathbf{R}(\cdot)$ and $R(\cdot)$ are the stability functions defined in (17) and (18), respectively. For any $x > 0$, we apply the eigenvalue decomposition (26) to estimate

$$\|\mathbf{A}^{-1}(\mathbf{I} + \tau_j x \mathbf{A})^{-1}\| \leq \|\mathbf{A}^{-1}\| \|(\mathbf{I} + \tau_j x \mathbf{A})^{-1}\| \leq \frac{\max_{1 \leq i \leq s} \{|\lambda_i^{-1}|\}}{1 + \min_{1 \leq i \leq s} \{\operatorname{Re} \lambda_i\} \tau_j x},$$

and

$$\left\| \mathbf{R}(-\tau_n x) \mathbf{e}_s^\top \right\| = \left\| (\mathbf{I} + \tau_n \mathbf{A} x)^{-1} \mathbf{1} \mathbf{e}_s^\top \right\| \leq \|(\mathbf{I} + \tau_n \mathbf{A} x)^{-1}\| \|\mathbf{1} \mathbf{e}_s^\top\| \leq \frac{\sqrt{s}}{1 + \min_{1 \leq i \leq s} \{\operatorname{Re} \lambda_i\} \tau_n x}.$$

Hence, it follows that

$$\|\mathbf{A}(\mathbf{I} + \tau_j x \mathbf{A})^{-1}\| \left\| \mathbf{R}(-\tau_n x) \mathbf{e}_s^\top \right\| \leq \frac{\sqrt{s} \max_{1 \leq i \leq s} \{|\lambda_i^{-1}|\}}{1 + \min_{1 \leq i \leq s} \{\operatorname{Re} \lambda_i\} (\tau_n + \tau_j) x}, \quad n \geq j, \quad j \geq 1.$$

In addition, Lemma 7 provides the product estimate

$$\left| \prod_{l=j+1}^{n-1} R(-\tau_l x) \right| \leq \frac{1}{1 + \hat{b}(t_{n-1} - t_j)}, \quad n \geq j, \quad j \geq 1.$$

Let

$$\hat{v} = \min \left\{ \hat{b}, \min_{1 \leq i \leq s} \{\operatorname{Re} \lambda_i\} \right\}.$$

By combining these estimates and employing the Beta function identity (89), we establish

$$\begin{aligned} \|\mathbf{W}_{n,j}\| &\leq \frac{M\tau_j}{\pi} \left(\int_0^\infty x^{-\alpha} \frac{\sqrt{s} \max_{1 \leq i \leq s} \{|\lambda_i^{-1}|\}}{1 + \hat{v}(t_n - t_{j-1})x} dx \right) \\ &= \frac{M\tau_j}{\pi} \sqrt{s} B(\alpha, 1 - \alpha) \max_{1 \leq i \leq s} \{|\lambda_i^{-1}|\} (\hat{v}(t_n - t_{j-1}))^{\alpha-1}. \end{aligned}$$

The proof is thus complete. \square

The stability of scheme (21) follows directly from the preceding weight estimates, as formalized in the following theorem.

Theorem 9. *Under Assumptions 1 and 2, the Runge–Kutta based gCQ scheme (21) satisfies*

$$\|u_n\|_{\mathcal{Y}} \leq CM \sum_{j=1}^n \tau_j (t_n - t_{j-1})^{\alpha-1} \|f_j\|_{C^0([t_{j-1}, t_j]; \mathcal{X})}.$$

4 Proof of Theorems 4 and 5

Following Lubich’s operational framework [25], we adopt the following notation for the error analysis:

$K(\partial_t)f := k * f$, the continuous convolution defined in (1),

$K(\partial_t^\Delta)f$, the Runge–Kutta based gCQ approximation of (1) on the time mesh Δ .

4.1 Error representation on the real axis

Let $\mathbf{Y}(x, t_n) := (y(x, t_{n-1} + c_i \tau_n))_{i=1}^s$. Substituting the exact solution into the Runge–Kutta scheme (15) gives

$$\mathbf{Y}(x, t_n) = y(x, t_{n-1})\mathbb{1} + \tau_n \mathbf{A}(-x\mathbf{Y}(x, t_n) + \mathbf{f}_n) + \mathbf{D}_n(x), \quad \text{for } n \geq 1, \quad (31a)$$

$$y(x, t_n) = y(x, t_{n-1}) + \tau_n \mathbf{b}^\top (-x\mathbf{Y}(x, t_n) + \mathbf{f}_n) + d_n(x), \quad \text{for } n \geq 1, \quad (31b)$$

where $\mathbf{D}_n = (d_{ni})_{i=1}^s$ and d_n denote the defects. Under Assumption 2, these defects admit the representations [29, proof of Theorem 3.3]:

$$d_{ni}(x) = \sum_{\ell=q+1}^p \delta_i^{(\ell)} \tau_n^\ell \frac{\partial^\ell y}{\partial t^\ell}(x, t_n) + \tau_n^p \int_{t_{n-1}}^{t_n} \kappa_i \left(\frac{t - t_{n-1}}{\tau_n} \right) \frac{\partial^{p+1} y}{\partial t^{p+1}} dt, \quad (32)$$

$$d_n(x) = \tau_n^p \int_{t_{n-1}}^{t_n} \kappa \left(\frac{t - t_{n-1}}{\tau_n} \right) \frac{\partial^{p+1} y}{\partial t^{p+1}} dt, \quad (33)$$

where κ_i and κ are bounded Peano kernels, and

$$\delta_i^{(\ell)} = \left(\frac{c_i^\ell}{\ell} - \sum_{j=1}^s a_{ij} c_j^{\ell-1} \right) / (\ell-1)!. \quad (34)$$

Denote $\mathbf{E}_n(x) := \mathbf{Y}(x, t_n) - \mathbf{Y}_n(x)$ and $e_n(x) := y(x, t_n) - y_n(x)$. Subtracting (15) from (31) gives

$$\begin{aligned} \mathbf{E}_n(x) &= e_{n-1}(x) \mathbb{1} - \tau_n x \mathbf{A} \mathbf{E}_n(x) + \mathbf{D}_n(x), \quad \text{for } n \geq 1, \\ e_n(x) &= e_{n-1}(x) - \tau_n x \mathbf{b}^\top \mathbf{E}_n(x) + d_n(x), \quad \text{for } n \geq 1. \end{aligned} \quad (35)$$

Solving the recursion (35), we obtain

$$e_n(x) = \sum_{j=1}^n \left(d_j(x) - \tau_j x \mathbf{b}^\top (\mathbf{I} + \tau_j x \mathbf{A})^{-1} \mathbf{D}_j(x) \right) \prod_{l=j+1}^n R(-\tau_l x), \quad (36)$$

with $e_0(x) = 0$ and $R(z)$ defined in (18). Then, the error representation of the Runge–Kutta based gCQ scheme (21) can be expressed as

$$u(t_n) - u_n = \int_0^\infty G(x) e_n(x) dx := \mathcal{E}_n^1 + \mathcal{E}_n^2, \quad (37)$$

where

$$\mathcal{E}_n^1 = \int_0^\infty G(x) \left(d_1(x) - \tau_1 x \mathbf{b}^\top (\mathbf{I} + \tau_1 x \mathbf{A})^{-1} \mathbf{D}_1(x) \right) \left(\prod_{j=2}^n R(-\tau_j x) \right) dx, \quad (38)$$

$$\mathcal{E}_n^2 = \sum_{j=2}^n \int_0^\infty G(x) \left(d_j(x) - \tau_j x \mathbf{b}^\top (\mathbf{I} + \tau_j x \mathbf{A})^{-1} \mathbf{D}_j(x) \right) \left(\prod_{l=j+1}^n R(-\tau_l x) \right) dx. \quad (39)$$

4.2 Convergence analysis for power-type integrands

To establish error estimates for general integrands f satisfying (12), we begin by analyzing the case $f(t) = t^\beta \mathbf{v}$ with $\beta > -1$. The error analysis proceeds by examining each component of the error decomposition (37) on the general mesh (2).

4.2.1 Error estimate for the first time interval

Lemma 10. *Let $\beta > -1$ and $x > 0$. Under Assumption 2, the defects in (31a) with $f(t) = t^\beta \mathbf{v}$ and $n = 1$ satisfy*

$$\max_{1 \leq i \leq s} \|d_{1i}(x)\|_{\mathcal{X}} \leq C\Gamma(\beta+1)\tau_1^{\beta+1} \begin{cases} \frac{1}{1+x c_1 \tau_1}, & \text{if } c_1 > 0, \\ \frac{1}{1+x c_2 \tau_1}, & \text{if } c_1 = 0, \quad \beta > 0, \end{cases} \quad (40)$$

where c_i denotes the i th component of the vector \mathbf{c} in the Butcher tableau, with $0 \leq c_1 \leq c_2 \leq \dots \leq c_s = 1$.

Proof. By (31a), we have

$$\|d_{1i}\|_{\mathcal{X}} = \left\| y(x, c_i \tau_1) - \tau_1 \sum_{j=1}^s a_{ij} y_t(x, c_j \tau_1) \right\|_{\mathcal{X}}.$$

Note that when $c_1 = 0$, the condition $\beta > 0$ is required to ensure boundedness of $y_t(x, 0)$. Applying (90), the estimate (40) follows. \square

Lemma 11. Under Assumption 2, for $\tau > 0$, $x > 0$, and $\delta^{(\ell)}$ defined in (34) with $q + 1 \leq \ell \leq p$, it holds

$$\left| \tau x \mathbf{b}^\top (\mathbf{I} + \tau x \mathbf{A})^{-1} \delta^{(\ell)} \right| \leq \begin{cases} C(\tau x)^{p-\ell+1}, & 0 < x < (\tau \|\mathbf{A}\|)^{-1}, \\ C, & x \geq (\tau \|\mathbf{A}\|)^{-1}, \end{cases} \quad (41)$$

where $C > 0$ is a constant independent of τ and x , and $\|\mathbf{A}\|$ denotes the induced matrix norm.

Proof. We first establish a uniform bound valid for all $x > 0$, then refine it for small x . From the stiff accuracy condition (10) and the eigendecomposition (26), we have

$$\left\| \tau x \mathbf{b}^\top (\mathbf{I} + \tau x \mathbf{A})^{-1} \right\| = \left\| \mathbf{e}_s^\top - \mathbf{e}_s^\top (\mathbf{I} + \tau x \mathbf{A})^{-1} \right\| \leq 1 + \frac{1}{1 + \tau x \lambda_{\min}} \leq 2, \quad (42)$$

where λ_{\min} is given in (27). Thus, for any $x > 0$

$$\left| \tau x \mathbf{b}^\top (\mathbf{I} + \tau x \mathbf{A})^{-1} \delta^{(\ell)} \right| \leq 2 \left\| \delta^{(\ell)} \right\| \leq C.$$

When $0 < x < (\tau \|\mathbf{A}\|)^{-1}$, the Neumann series expansion gives

$$(\mathbf{I} + \tau x \mathbf{A})^{-1} = \sum_{m=0}^{\infty} (-\tau x \mathbf{A})^m.$$

Together with the order conditions

$$\mathbf{b}^\top \mathbf{A}^{m+1} \mathbf{c}^{\ell-1} = \frac{1}{\ell} \mathbf{b}^\top \mathbf{A}^m \mathbf{c}^\ell \quad \text{for } m + 1 + \ell \leq p,$$

and the definition of $\delta^{(\ell)}$ in (34), it follows for each $q + 1 \leq \ell \leq p$ that

$$\left| \tau x \mathbf{b}^\top (\mathbf{I} + \tau x \mathbf{A})^{-1} \delta^{(\ell)} \right| = \left| \tau x \mathbf{b}^\top \sum_{m=p-\ell}^{\infty} (-\tau x \mathbf{A})^m \delta^{(\ell)} \right| \leq C(\tau x)^{p-\ell+1}.$$

This completes the proof. \square

We now establish the error bound for \mathcal{E}_n^1 in (38).

Lemma 12. Given $f(t) = t^\beta \mathbf{v}$ with $\beta > -1$, under Assumptions 1 and 2, the approximation error \mathcal{E}_n^1 in (38) on the mesh (2) satisfies

$$\|\mathcal{E}_n^1\|_{\mathcal{Y}} \leq CM \tau_1^{\alpha+\beta}, \quad (43)$$

where the positive constant C is independent of the mesh.

Proof. Using (5) and the bound (9), it follows that

$$\|\mathcal{E}_n^1\|_{\mathcal{Y}} \leq CM \int_0^\infty x^{-\alpha} \left(\|d_1(x)\|_{\mathcal{X}} + \left\| \tau_1 x \mathbf{b}^\top (\mathbf{I} + \tau_1 x \mathbf{A})^{-1} \mathbf{D}_1(x) \right\|_{\mathcal{X}} \right) dx.$$

The bound in (42) simplifies this to

$$\|\mathcal{E}_n^1\|_{\mathcal{Y}} \leq CM \int_0^\infty x^{-\alpha} \max_{1 \leq i \leq s} \|d_{1i}(x)\|_{\mathcal{X}} dx.$$

Applying Lemma 10 with the integral identity (89), we derive

$$\|\mathcal{E}_n^1\|_{\mathcal{Y}} \leq CM \tau_1^{\beta+1} \int_0^\infty x^{-\alpha} \frac{1}{1 + \tilde{c} t_1 x} dx = CMB(\alpha, 1 - \alpha) \tilde{c}^{\alpha-1} \tau_1^{\alpha+\beta},$$

where

$$\tilde{c} = \begin{cases} c_1, & \text{if } c_1 \neq 0 \text{ and } \beta > -1, \\ c_2, & \text{if } c_1 = 0 \text{ and } \beta > 0. \end{cases} \quad (44)$$

\square

4.2.2 Error estimates from the second time interval

This subsection focuses on establishing an error bound for the accumulated error \mathcal{E}_n^2 defined in (39), for $n \geq 2$. The analysis begins with the following lemma.

Lemma 13. *For the defects $d_j(x)$ in (31) with $f(t) = t^\beta \mathbf{v}$, where $\beta > -1$, the following bound holds on the general mesh (2):*

$$\sum_{j=2}^n \int_0^\infty x^{-\alpha} \|d_j(x)\|_{\mathcal{X}} dx \leq C \begin{cases} \tau_{\max}^p t_n^{\alpha+\beta-p}, & \text{if } \beta > p - \alpha, \\ |\log(t_n/t_1)| \tau_{\max}^p, & \text{if } \beta = p - \alpha, \\ \sum_{j=2}^n \tau_j^{p+1} \xi_j^{\alpha+\beta-p-1}, & \text{if } \beta < p - \alpha, \end{cases} \quad (45)$$

where $\xi_j \in (t_{j-1}, t_j)$ and C is a positive constant independent of the mesh.

Proof. Using (33), we have

$$\sum_{j=2}^n \int_0^\infty x^{-\alpha} \|d_j(x)\|_{\mathcal{X}} dx \leq C \int_0^\infty x^{-\alpha} \left(\sum_{j=2}^n \tau_j^p \int_{t_{j-1}}^{t_j} \left\| \frac{\partial^{p+1} y}{\partial t^{p+1}} \right\|_{\mathcal{X}} dt \right) dx.$$

From (90), it follows that

$$\sum_{j=2}^n \tau_j^p \int_{t_{j-1}}^{t_j} \left\| \frac{\partial^{p+1} y(t)}{\partial t^{p+1}} \right\|_{\mathcal{X}} dt \leq C\Gamma(\beta+1) \sum_{j=2}^n \tau_j^p \int_{t_{j-1}}^{t_j} \frac{t^{\beta-p}}{1+xt} dt, \quad \text{for } x > 0. \quad (46)$$

Hence,

$$\int_0^\infty x^{-\alpha} \|d_j(x)\|_{\mathcal{X}} dx \leq C\Gamma(\beta+1) \sum_{j=2}^n \tau_j^p \int_{t_{j-1}}^{t_j} t^{\beta-p} \left(\int_0^\infty \frac{x^{-\alpha}}{1+xt} dx \right) dt.$$

By applying the definition of the Beta function given in (89), we derive

$$\int_0^\infty x^{-\alpha} \|d_j(x)\|_{\mathcal{X}} dx \leq C\Gamma(\beta+1)B(\alpha, 1-\alpha) \sum_{j=2}^n \tau_j^p \int_{t_{j-1}}^{t_j} t^{\alpha+\beta-p-1} dt.$$

The final bound (45) is obtained through direct integration, thereby completing the proof. \square

Lemma 14. *Suppose the s -stage Runge-Kutta method satisfies Assumption 2. Define*

$$P_j := \sum_{\ell=q+1}^p \int_0^\infty x^{-\alpha} \left\| \tau_j x \mathbf{b}^\top (\mathbf{I} + \tau_j x \mathbf{A})^{-1} \delta^{(\ell)} \tau_j^\ell \frac{\partial^\ell y}{\partial t^\ell}(x, t_j) \right\|_{\mathcal{X}} \prod_{l=j+1}^n |R(-\tau_l x)| dx, \quad (47)$$

for $2 \leq j \leq n$, where $y(x, t)$ is the solution to (11) with $f(t) = t^\beta \mathbf{v}$, $\beta > -1$. Then, on the general time mesh (2), it holds

$$\sum_{j=2}^n P_j \leq C |\log(\tau_n)| \begin{cases} \tau_{\max}^{\min\{p, q+1+\alpha\}} t_n^{\alpha+\beta-\min\{p, q+1+\alpha\}}, & \text{if } \beta \geq p - \alpha, \\ \max_{2 \leq j \leq n} \left\{ \tau_j^{q+1+\alpha} t_j^{\beta-q-1} + \tau_j^p t_j^{\alpha+\beta-p} \right\}, & \text{if } \beta < p - \alpha, \end{cases} \quad (48)$$

where C is a positive constant independent of the mesh.

Proof. By Lemma 7 and the estimate in (90), we have

$$P_j \leq C \sum_{\ell=q+1}^p \tau_j^\ell t_j^{\beta-\ell+1} \int_0^\infty x^{-\alpha} \left| \tau_j x \mathbf{b}^\top (\mathbf{I} + \tau_j x \mathbf{A})^{-1} \delta^{(\ell)} \right| \frac{1}{(1+t_j x)(1+\hat{b}(t_n-t_j)x)} dx.$$

For the case $j = n$, Lemma 11 yields

$$\begin{aligned} P_n \leq & C \sum_{\ell=q+1}^{p-1} \left(\tau_n^{p+1} t_n^{\beta-\ell+1} \int_0^{1/(\tau_n \|\mathbf{A}\|)} \frac{x^{-\alpha+p-\ell+1}}{1+t_n x} dx + \tau_n^\ell t_n^{\beta-\ell+1} \int_{1/(\tau_n \|\mathbf{A}\|)}^\infty \frac{x^{-\alpha}}{1+t_n x} dx \right) \\ & + C \tau_n^p t_n^{\beta-p+1} \int_0^\infty \frac{x^{-\alpha}}{1+t_n x} dx, \end{aligned}$$

which gives

$$P_n \leq C \sum_{\ell=q+1}^{p-1} \tau_n^{\alpha+\ell} t_n^{\beta-\ell} + C \tau_n^p t_n^{\alpha+\beta-p}. \quad (49)$$

Using

$$\tau_j/t_j < 1 \quad \text{for all } j \geq 2, \quad (50)$$

we further deduce that

$$P_n \leq C \left(\tau_n^{q+1+\alpha} t_n^{\beta-q-1} + \tau_n^p t_n^{\alpha+\beta-p} \right).$$

Now consider the case $2 \leq j \leq n-1$. In this case, we have

$$P_j \leq C \sum_{\ell=q+1}^p \tau_j^\ell (\hat{b}(t_n-t_j))^{-1} t_j^{\beta-\ell+1} \int_0^\infty x^{-\alpha-1} \left| \tau_j x \mathbf{b}^\top (\mathbf{I} + \tau_j x \mathbf{A})^{-1} \delta^{(\ell)} \right| \frac{1}{1+t_j x} dx.$$

Applying Lemma 11 gives

$$P_j \leq C \sum_{\ell=q+1}^p \left(|I_{\text{near}}^{(\ell)}| + \tau_j^{\alpha+\ell+1} (\hat{b}(t_n-t_j))^{-1} t_j^{\beta-\ell} \right), \quad (51)$$

where

$$I_{\text{near}}^{(\ell)} := \tau_j^{p+1} (\hat{b}(t_n-t_j))^{-1} t_j^{\beta-\ell+1} \int_0^{1/(\tau_j \|\mathbf{A}\|)} x^{-\alpha+p-\ell} \frac{1}{1+t_j x} dx.$$

Evaluating the integral explicitly yields

$$|I_{\text{near}}^{(\ell)}| \leq \begin{cases} C \tau_j^{\alpha+\ell+1} (\hat{b}(t_n-t_j))^{-1} t_j^{\beta-\ell}, & q+1 \leq \ell \leq p-1, \\ B(\alpha, 1-\alpha) \tau_j^{p+1} (\hat{b}(t_n-t_j))^{-1} t_j^{\alpha+\beta-p}, & \ell = p. \end{cases} \quad (52)$$

Substituting (52) into (51), we obtain

$$\begin{aligned} P_j & \leq C \sum_{\ell=q+1}^{p-1} \tau_j^{\alpha+\ell+1} (\hat{b}(t_n-t_j))^{-1} t_j^{\beta-\ell} + C \tau_j^{p+1} (\hat{b}(t_n-t_j))^{-1} t_j^{\alpha+\beta-p} \\ & \leq C (\hat{b}(t_n-t_j))^{-1} \left(\tau_j^{q+2+\alpha} t_j^{\beta-q-1} + \tau_j^{p+1} t_j^{\alpha+\beta-p} \right), \end{aligned} \quad (53)$$

where (50) is applied in the last step. Combining all cases yields

$$\sum_{j=2}^n P_j \leq C \left(1 + \sum_{j=2}^{n-1} \tau_j (\hat{b}(t_n-t_j))^{-1} \right) \max_{2 \leq j \leq n} \left\{ \tau_j^{q+1+\alpha} t_j^{\beta-q-1} + \tau_j^p t_j^{\alpha+\beta-p} \right\}.$$

Using the inequality

$$1 + \sum_{j=2}^{n-1} \tau_j (\hat{b}(t_n - t_j))^{-1} \leq 1 + \hat{b}^{-1} + \hat{b}^{-1} \int_0^{t_{n-1}} (t_n - s)^{-1} ds \leq C |\log(\tau_n)|, \quad (54)$$

we have

$$\sum_{j=2}^n P_j \leq C |\log(\tau_n)| \max_{2 \leq j \leq n} \left\{ \tau_j^{q+1+\alpha} t_j^{\beta-q-1} + \tau_j^p t_j^{\alpha+\beta-p} \right\}.$$

Furthermore, application of (50) gives

$$\tau_j^{q+1+\alpha} t_j^{\beta-q-1} + \tau_j^p t_j^{\alpha+\beta-p} < 2 \tau_j^{\min\{p, q+1+\alpha\}} t_j^{\alpha+\beta-\min\{p, q+1+\alpha\}}, \quad \text{for all } 2 \leq j \leq n. \quad (55)$$

Thus we can get (48), which completes the proof. \square

Lemma 15. *Let the right-hand side term in (11) be $f(t) = t^\beta \mathbf{v}$ with $\beta > -1$. Under Assumptions 1 and 2, for the error term \mathcal{E}_n^2 defined in (39) on the general time mesh (2), it holds that*

$$\begin{aligned} \|\mathcal{E}_n^2\|_{\mathcal{Y}} &\leq \\ CM &\begin{cases} |\log(\tau_{\min})| \tau_{\max}^{\min\{p, q+1+\alpha\}}, & \text{if } \beta \geq p - \alpha, \\ \sum_{j=2}^n \tau_j^{p+1} \xi_j^{\alpha+\beta-p-1} + |\log(\tau_n)| \max_{2 \leq j \leq n} \left\{ \tau_j^{q+1+\alpha} t_j^{\beta-q-1} + \tau_j^p t_j^{\alpha+\beta-p} \right\}, & \text{if } \beta < p - \alpha. \end{cases} \end{aligned} \quad (56)$$

where $\xi_j \in (t_{j-1}, t_j)$, the positive constant C is independent of the mesh (2).

Proof. From the definition of \mathcal{E}_n^2 in (39), together with (5) and (29), it follows that

$$\begin{aligned} \|\mathcal{E}_n^2\|_{\mathcal{Y}} &\leq CM \sum_{j=2}^n \left(\int_0^\infty x^{-\alpha} \|d_j(x)\|_{\mathcal{X}} \left| \prod_{l=j+1}^n R(-\tau_l x) \right| dx + P_j \right) \\ &\leq CM \sum_{j=2}^n \left(\int_0^\infty x^{-\alpha} \|d_j(x)\|_{\mathcal{X}} dx + P_j \right), \end{aligned} \quad (57)$$

where d_j is the defect in (33), P_j is defined in (47). Applying Lemmas 13 and 14 to (57) yields the estimate (56), completing the proof. \square

Combining Lemmas 12 and 15, the convergence results for $f(t) = t^\beta \mathbf{v}$ is stated as below.

Proposition 16. *Assume that $K(z)$ satisfies Assumption 1 and the Runge–Kutta method satisfies Assumption 2. Given the general time mesh (2), the error of the Runge–Kutta based gCQ approximation (21) applied to (1) with $f(t) = t^\beta \mathbf{v}$ ($\beta > -1$) satisfies*

$$\begin{aligned} \|u(t_n) - u_n\|_{\mathcal{Y}} &\leq \\ CM &\begin{cases} |\log(\tau_{\min})| \tau_{\max}^{\min\{p, q+1+\alpha\}}, & \text{if } \beta \geq p - \alpha, \\ \sum_{j=2}^n \tau_j^{p+1} \xi_j^{\alpha+\beta-p-1} + |\log(\tau_n)| \max_{1 \leq j \leq n} \left\{ \tau_j^{q+1+\alpha} t_j^{\beta-q-1} + \tau_j^p t_j^{\alpha+\beta-p} \right\}, & \text{if } \beta < p - \alpha, \end{cases} \end{aligned} \quad (58)$$

where $n \geq 1$, $\xi_j \in (t_{j-1}, t_j)$, C is a positive constant independent of the time mesh (2).

Below we derive specific error estimates for two especial cases: the case of quasi-uniform meshes like in (13) and, among them, the case of graded meshes (14). For general quasi-uniform meshes we can relax the requirement about the number of vanishing moments at the origin, whereas for graded meshes we do not need to assume any of them, since we can always achieve full order of convergence by choosing properly the grading parameter.

Corollary 17. *Under the assumptions in Proposition 16, the following error estimates hold for $f(t) = t^\beta \mathbf{v}$.*

- (i) *If the mesh is quasi-uniform as in (13), we can relax the condition on β in (58) to $\beta \geq \min\{p - \alpha, q + 1\}$, and the error is bounded by*

$$\|u(t_n) - u_n\|_{\mathcal{Y}} \leq CM c_{\Delta}^{\max\{0, p-q-\alpha\}} |\log(\tau_{\min})| \tau_{\max}^{\min\{p, q+1+\alpha\}}, \quad n \geq 1. \quad (59)$$

- (ii) *For any $\beta > -1$, the error on the graded mesh (14) can be estimated by*

$$\|u(t_n) - u_n\|_{\mathcal{Y}} \leq CM \log(N) \begin{cases} N^{-\gamma(\alpha+\beta)}, & \gamma(\alpha+\beta) < \min\{p, q+1+\alpha\}, \\ N^{-\min\{p, q+1+\alpha\}}, & \gamma(\alpha+\beta) \geq \min\{p, q+1+\alpha\}, \end{cases}$$

where $1 \leq n \leq N$, C is independent of N .

Proof. When $\beta \geq p - \alpha$, the results in Cases (i) and (ii) follow directly from Proposition 16.

For Case (i), it remains to derive the error bound under the condition

$$\beta \geq q + 1 \quad \text{with} \quad q + 1 = \min\{p - \alpha, q + 1\}. \quad (60)$$

We begin by analyzing the summation in (58). The quasi-uniformity property of the mesh (13) implies the lower bound

$$t_{j-1} = \sum_{\ell=1}^{j-1} \tau_{\ell} > \sum_{\ell=1}^{j-1} \frac{\tau_{\ell}}{2} + \frac{\tau_j}{4c_{\Delta}} \geq \frac{t_j}{4c_{\Delta}}.$$

Applying this bound to the summation in (56) yields

$$\begin{aligned} \sum_{j=2}^n \tau_j^{p+1} \xi_j^{\alpha+\beta-p-1} &\leq (4c_{\Delta})^{\max\{0, p+1-\alpha-\beta\}} \sum_{j=2}^n \tau_j^{p+1} t_j^{\alpha+\beta-p-1} \\ &\leq (4c_{\Delta})^{\max\{0, p+1-\alpha-\beta\}} \left(\sum_{j=2}^n \tau_j t_j^{-1} \right) \max_{2 \leq j \leq n} \left\{ \tau_j^p t_j^{\alpha+\beta-p} \right\}. \end{aligned}$$

Using the integral estimate

$$\sum_{j=2}^n \tau_j t_j^{-1} < 1 + \int_{t_1}^{t_n} t^{-1} dt = 1 + \log(t_n/t_1)$$

along with (55) and (60), we obtain

$$\sum_{j=2}^n \tau_j^{p+1} \xi_j^{\alpha+\beta-p-1} \leq C c_{\Delta}^{\max\{0, p-q-\alpha\}} |\log(\tau_1)| \tau_{\max}^{q+1+\alpha} t_n^{\beta-q-1}. \quad (61)$$

Substituting the bound above into (56) and then applying (55) completes the proof of Case (i).

For case (ii), the bound (58) with $\beta \leq p - \alpha$ on the graded mesh (14) satisfies

$$\|u(t_n) - u_n\|_{\mathcal{Y}} \leq CM \left(\sum_{j=2}^n \tau_j^{p+1} \xi_j^{\alpha+\beta-p-1} + \log(N) \max_{1 \leq j \leq n} \left\{ \tau_j^{q+1+\alpha} t_j^{\beta-q-1} + \tau_j^p t_j^{\alpha+\beta-p} \right\} \right).$$

Applying (93) gives

$$\sum_{j=2}^n \tau_j^{p+1} \xi_j^{\alpha+\beta-p-1} \leq C \begin{cases} N^{-\gamma(\alpha+\beta)}, & \gamma(\alpha+\beta) < p, \\ N^{-p} \log(n), & \gamma(\alpha+\beta) = p, \\ N^{-p} t_n^{\alpha+\beta-p/\gamma}, & \gamma(\alpha+\beta) > p. \end{cases}$$

Next, using (92), we can derive

$$\begin{aligned} & \tau_j^{q+1+\alpha} t_j^{\beta-q-1} + \tau_j^p t_j^{\alpha+\beta-p} \\ & \leq C \begin{cases} N^{-\gamma(\alpha+\beta)}, & \text{if } \gamma(\alpha+\beta) < \min\{p, q+1+\alpha\}, \\ N^{-\min\{p, q+1+\alpha\}} t_j^{\alpha+\beta-\min\{p, q+1+\alpha\}/\gamma}, & \text{if } \gamma(\alpha+\beta) \geq \min\{p, q+1+\alpha\}. \end{cases} \end{aligned}$$

Combining these estimates proves (ii). \square

4.3 Convergence analysis for general integrands

Lemma 18. *Let $y(x, t)$ be the solution to (11) with right-hand side given by*

$$f(t) = H(t - \eta)(t - \eta)^\beta \mathbf{v}, \quad \eta \geq 0, \quad (62)$$

where $H(\cdot)$ is the Heaviside step function and $\mathbf{v} \in \mathcal{X}$. Let $d_j(x)$ denote the associated defect in (31). Under Assumptions 1 with $\beta \geq p - 1 \geq 0$, for $2 \leq j \leq n - 1$, it holds that

$$\|d_j(x)\|_{\mathcal{X}} \left| \prod_{l=j+1}^n R(-\tau_l x) \right| \leq C \tau_j^p \begin{cases} t_j^{\beta-p+1} \int_{t_{j-1}}^{t_j} \frac{1}{(t - \eta)(1 + \hat{b}(t_n - t_j)x)} dt, & \eta \in [0, t_{j-1}), \\ (1 + \hat{b}(t_n - t_j)x)^{-1}, & \eta \in [t_{j-1}, t_j], \\ 0, & \eta \in (t_j, \infty). \end{cases}$$

Moreover, for $j = n$, we have

$$\|d_n(x)\|_{\mathcal{X}} \leq C \tau_n^p \begin{cases} t_n^{\beta-p+1} \int_{t_{n-1}}^{t_n} \frac{1}{(t - \eta)(1 + (t - \eta)x)} dt, & \eta \in [0, t_{n-1}), \\ \|H(t_{n-1} + \mathbf{c}\tau_n - \eta)(1 + (t_{n-1} + \mathbf{c}\tau_n - \eta)x)^{-1}\|_{\infty}, & \eta \in [t_{n-1}, t_n], \\ 0, & \eta \in (t_n, \infty), \end{cases}$$

where $\mathbf{c} = (c_i)_{i=1}^s$ represents the abscissae from the Butcher tableau, C and \hat{b} are positive constants independent of the mesh.

Proof. From the representation in (31), the defect $d_j(x)$ can be expressed as

$$d_j(x) = \begin{cases} \tau_j^p \int_{t_{j-1}}^{t_j} \kappa\left(\frac{t - t_{j-1}}{\tau_j}\right) \frac{\partial^{p+1} y}{\partial t^{p+1}}(x, t) dt, & \eta \in [0, t_{j-1}), \\ y(x, t_j) - y(x, t_{j-1}) - \tau_j \mathbf{b}^\top \mathbf{Y}_t(x, t_j), & \eta \in [t_{j-1}, t_j], \\ 0, & \eta \in (t_j, \infty). \end{cases}$$

Applying (29) and (91), we obtain for $\eta \in [0, t_{j-1}]$:

$$\|d_j(x)\|_{\mathcal{X}} \left| \prod_{l=j+1}^n R(-\tau_l x) \right| \leq C\tau_j^p \int_{t_{j-1}}^{t_j} \frac{(t-\eta)^{\beta-p}}{(1+(t-\eta)x)(1+\hat{b}(t_n-t_j)x)} dt,$$

and for $\eta \in [t_{j-1}, t_j]$:

$$\|d_j(x)\|_{\mathcal{X}} \left| \prod_{l=j+1}^n R(-\tau_l x) \right| \leq C\tau_j^{\beta+1} \left\| \frac{H(t_{n-1} + \mathbf{c}\tau_n - \eta)}{(1+(t_{n-1} + \mathbf{c}\tau_n - \eta)x)(1+\hat{b}(t_n-t_j)x)} \right\|_{\infty},$$

where $\mathbf{c} = (c_i)_{i=1}^s$ denotes the vector of nodes in the Butcher tableau, and $\hat{b} > 0$ is the constant from (29). The final bounds then follow from using $\beta \geq p-1$ and

$$(t-\eta)^{\beta-p} \leq t_j^{\beta-p+1}/(t-\eta), \quad \text{for } t \in (t_{j-1}, t_j), \quad \eta \in (0, t_{j-1}), \quad 2 \leq j \leq n.$$

□

Lemma 19. *Let $y(x, t)$ be the solution to (11) with f given by (62), where $\beta \geq p-1 \geq 0$ and $0 < \alpha < 1$. Under Assumptions 1 and 2, the following estimates hold:*

$$\|\mathcal{E}_n^1\|_{\mathcal{Y}} \leq CM\tau_1 H(\tau_1 - \eta)(\tau_1 - \eta)^{\alpha+\beta-1},$$

and

$$\sum_{j=2}^n P_j \leq C|\log(\tau_n)| \left(\tau_{\max}^{q+1+\alpha} + \tau_{\max}^p \max_{2 \leq j \leq n} \left\{ H(t_j - \eta)(t_j - \eta)^{\alpha+\beta-p} \right\} \right),$$

where \mathcal{E}_n^1 denotes the approximation error defined in (38), and P_j is given by (47).

Proof. Applying the derivative bound (91) to the defects \mathbf{D}_1 in (31a) yields

$$\max_{1 \leq i \leq s} \|d_{1i}(x)\|_{\mathcal{X}} \leq C\Gamma(\beta+1)\tau_1 H(t_1 - \eta)(t_1 - \eta)^{\beta}.$$

Following the proof of Lemma 12, we obtain the stated bound for $\|\mathcal{E}_n^1\|_{\mathcal{Y}}$.

For P_j in (47), adapting the proofs of (49) and (53) and applying (91) yields

$$\begin{aligned} P_n &\leq CH(t_n - \eta) \left(\sum_{\ell=q+1}^{p-1} \tau_n^{\alpha+\ell} (t_n - \eta)^{\beta-\ell} + \tau_n^p (t_n - \eta)^{\alpha+\beta-p} \right), \\ P_j &\leq CH(t_j - \eta) \sum_{\ell=q+1}^{p-1} \tau_j^{\alpha+\ell+1} (\hat{b}(t_n - t_j))^{-1} (t_j - \eta)^{\beta-\ell} \\ &\quad + CH(t_j - \eta) \tau_j^{p+1} (\hat{b}(t_n - t_j))^{-1} (t_j - \eta)^{\alpha+\beta-p}, \quad 2 \leq j \leq n-1. \end{aligned}$$

The final bound follows from these estimates by noting that $\beta \geq p-1$ and applying the logarithmic bound (54). □

Proposition 20. *Let the data f in (1) be given by*

$$f(t) = \frac{1}{\Gamma(m+\beta+1)} \left(t^{m+\beta} * f^{(m+\beta+1)} \right) (t), \quad (63)$$

where $\beta > -1$ and $m = \lceil p - \beta - 1 \rceil$. Under Assumptions 1 and 2, the error of the Runge-Kutta based gCQ approximation (21) on the general mesh (2) satisfies

$$\|u(t_n) - u_n\|_{\mathcal{Y}} \leq CM|\log(\tau_{\min})| \tau_{\max}^{\min\{p, q+1+\alpha\}} \left\| f^{(m+\beta+1)} \right\|_{C^0([0, t_n], \mathcal{X})}, \quad 1 \leq n \leq N, \quad (64)$$

where C is a constant independent of the temporal discretization (2).

Proof. Denote $(t - \eta)_+^{m+\beta} := H(t - \eta)(t - \eta)^{m+\beta}$. Following the argument in [14, Proposition 13], the continuous convolution and its Runge–Kutta based gCQ approximation, when applied to $f(t)$ in (63), can be represented as

$$[K(\partial_t)f](t_n) = \int_0^{t_n} \frac{f^{(m+\beta+1)}(\eta)}{\Gamma(m+\beta+1)} [K(\partial_t)(\cdot - \eta)_+^{m+\beta}](t_n) d\eta,$$

and

$$[K(\partial_t^\Delta)f]_n = \int_0^{t_n} \frac{f^{(m+\beta+1)}(\eta)}{\Gamma(m+\beta+1)} [K(\partial_t^\Delta)(\cdot - \eta)_+^{m+\beta}]_n d\eta.$$

The approximation error then satisfies

$$\begin{aligned} & \| [K(\partial_t)f](t_n) - [K(\partial_t^\Delta)f]_n \|_Y \\ &= \left\| \int_0^{t_n} \frac{f^{(m+\beta+1)}(\eta)}{\Gamma(m+\beta+1)} \left([K(\partial_t)(\cdot - \eta)_+^{m+\beta}](t_n) - [K(\partial_t^\Delta)(\cdot - \eta)_+^{m+\beta}]_n \right) d\eta \right\|_Y \\ &\leq \int_0^{t_n} \left\| [K(\partial_t)(\cdot - \eta)_+^{m+\beta}](t_n) - [K(\partial_t^\Delta)(\cdot - \eta)_+^{m+\beta}]_n \right\|_Y d\eta \cdot \|f^{(m+\beta+1)}\|_{C^0([0, t_n], \mathcal{X})}. \end{aligned}$$

Let $y(x, t)$ be the solution to (11) with right hand side $(t - \eta)_+^{m+\beta}$, and let $e_n(x)$ denote the associated Runge-Kutta approximation error from (36). Combining the error representation in (37) with the bound from (57), we obtain

$$\begin{aligned} & \int_0^{t_n} \left\| [K(\partial_t)(\cdot - \eta)_+^{m+\beta}](t_n) - [K(\partial_t^\Delta)(\cdot - \eta)_+^{m+\beta}]_n \right\|_Y d\eta \\ &\leq \int_0^{t_n} \left[\|\mathcal{E}_n^1\|_Y + CM \sum_{j=2}^n \left(\int_0^\infty x^{-\alpha} \|d_j(x)\|_{\mathcal{X}} \left| \prod_{l=j+1}^n R(-\tau_l x) \right| dx + P_j \right) \right] d\eta. \quad (65) \end{aligned}$$

For $2 \leq j \leq n-1$, applying Lemma 18 under the condition $m + \beta \geq p-1$, we obtain

$$\begin{aligned} & \int_0^{t_n} \left(\int_0^\infty x^{-\alpha} \|d_j(x)\|_{\mathcal{X}} \left| \prod_{l=j+1}^n R(-\tau_l x) \right| dx \right) d\eta \\ &\leq C\tau_j^p \int_0^\infty \frac{x^{-\alpha}}{1 + \hat{b}(t_n - t_j)x} dx \left(\int_0^{t_{j-1}} \int_{t_{j-1}}^{t_j} \frac{1}{t - \eta} dt d\eta + \tau_j \right) \\ &\stackrel{(89)}{=} C\tau_j^p (\hat{b}(t_n - t_j))^{\alpha-1} \left(\int_0^{t_{j-1}} \int_{t_{j-1}}^{t_j} \frac{1}{t - \eta} dt d\eta + \tau_j \right). \end{aligned}$$

For the integral term, we have

$$\begin{aligned} & \int_0^{t_{j-1}} \int_{t_{j-1}}^{t_j} \frac{1}{t - \eta} dt d\eta = t_j \log(t_j) - \tau_j \log(\tau_j) - t_{j-1} \log(t_{j-1}) \\ &\leq \tau_j |\log(\tau_j)| + \tau_j (1 + \log(t_j)) \leq C |\log(\tau_{\min})| \tau_j. \end{aligned}$$

Thus, we can bound the summation w.r.t. j in (65) by

$$\begin{aligned} & \sum_{j=2}^{n-1} \int_0^{t_n} \left(\int_0^\infty x^{-\alpha} \|d_j(x)\|_{\mathcal{X}} \left| \prod_{l=j+1}^n R(-\tau_l x) \right| dx \right) d\eta \\ &\leq C |\log(\tau_{\min})| \sum_{j=2}^{n-1} \tau_j^{p+1} (\hat{b}(t_n - t_j))^{\alpha-1} \leq C |\log(\tau_{\min})| \tau_{\max}^p t_n^\alpha. \quad (66) \end{aligned}$$

Now, for the term corresponding to $j = n$, applying Lemma 18 and (89), we get

$$\begin{aligned}
\int_0^{t_n} \int_0^\infty x^{-\alpha} \|d_n(x)\|_{\mathcal{X}} dx d\eta &\leq \tau_n^p \int_0^{t_{n-1}} \int_{t_{n-1}}^{t_n} (t - \eta)^{\alpha-2} dt d\eta \\
&+ C\tau_n^p \int_{t_{n-1}}^{t_n} \|H(t_{n-1} + \mathbf{c}\tau_n - \eta)(t_{n-1} + \mathbf{c}\tau_n - \eta)^{\alpha-1}\|_\infty d\eta \\
&\leq C\tau_n^p \int_0^{t_{n-1}} [(t_n - \eta)^{\alpha-1} - (t_{n-1} - \eta)^{\alpha-1}] d\eta + C\tau_n^{p+\alpha} \leq C\tau_n^p.
\end{aligned} \tag{67}$$

From (66) and (67), we can get that

$$\sum_{j=2}^n \int_0^{t_n} \left(\int_0^\infty x^{-\alpha} \|d_j(x)\|_{\mathcal{X}} \left| \prod_{l=j+1}^n R(-\tau_l x) \right| dx \right) d\eta \leq C |\log(\tau_{\min})| \tau_{\max}^p.$$

Applying Lemma 19 together with the bound above to (65) yields

$$\|u(t_n) - u_n\|_{\mathcal{Y}} \leq CM |\log \tau_{\min}| \tau_{\max}^{\min\{p, q+1+\alpha\}} \|f^{(m+\beta+1)}\|_{C^0([0, t_n], \mathcal{X})}.$$

□

Remark 21. By applying the bound (63) with $p = 1$ to the analysis of the Euler based gCQ method, we can relax the regularity condition in [14, Proposition 13] to data f in $C^1([0, T], \mathcal{X})$, rather than in $C^3([0, T], \mathcal{X})$.

By applying Proposition 16 and Proposition 20, we can establish the following convergence results for general integrands $f(t)$ of the form (12).

Proposition 22. Suppose that the transfer operator $K(z)$ satisfies Assumption 1 and the Runge–Kutta method satisfies Assumption 2. Let the integrand $f(t)$ in the convolution (1) take the form of (12) with $\beta > -1$ and $m = \lceil p - \beta - 1 \rceil$. Denote

$$\mu := \min\{p, q + 1 + \alpha\} \text{ and } \nu := \lceil p - \alpha - \beta - 1 \rceil.$$

Then, on the general mesh (2), it holds

$$\begin{aligned}
&\|u(t_n) - u_n\|_{\mathcal{Y}} \\
&\leq CM \sum_{\ell=0}^{\nu} \left(\sum_{j=2}^n \tau_j^{p+1} \xi_j^{\alpha+\beta+\ell-p-1} + |\log(\tau_n)| \max_{1 \leq j \leq n} \left\{ \tau_j^\mu t_j^{\alpha+\beta+\ell-\mu} \right\} \right) \|f^{(\ell+\beta)}(0)\|_{\mathcal{X}} \\
&+ CM |\log(\tau_{\min})| \tau_{\max}^\mu \left(\sum_{\ell=\nu+1}^m \|f^{(\ell+\beta)}(0)\|_{\mathcal{X}} + \|f^{(m+\beta+1)}\|_{C^0([0, t_n], \mathcal{X})} \right), \quad n \geq 1.
\end{aligned}$$

Here, $\xi_j \in (t_{j-1}, t_j)$ and the constant C is mesh-independent.

Remark 23. Proposition 22 directly implies the convergence result for general meshes, as stated in Case (i) of Theorem 4. For quasi-uniform meshes, the convergence result follows from Case (i) of Corollary 17, which is summarized as (ii) in Theorem 4. In the case of graded meshes, the corresponding convergence result is obtained via Case (ii) of Corollary 17, and is formally stated in Theorem 5.

5 Fast and oblivious Runge–Kutta gCQ

5.1 Algorithm for the convolution

For efficient implementation, we extend the algorithm proposed in [4] to the general mesh (2). Denoting

$$\mathbf{f}_n = (f(t_{n-1} + c_i \tau_n))_{i=1}^s, \quad 1 \leq n \leq N.$$

Following [14] and recalling the notation in (22), we split the gCQ approximation into two parts:

$$\mathbf{U}_n = [K(\partial_t^\Delta) \mathbf{f}]_n = \sum_{j=\max(1, n-n_0+1)}^n \mathbf{W}_{n,j} \mathbf{f}_j + \sum_{j=1}^{n-n_0} \mathbf{W}_{n,j} \mathbf{f}_j = \mathbf{S}_n^{loc} + \mathbf{S}_n^{his}, \quad (68)$$

with n_0 a fixed moderate constant, say $n_0 = 5$ and which can also be equal to 1. Using the definition of $\mathbf{W}_{n,j}$ in (23), we have

$$\begin{aligned} \mathbf{S}_n^{loc} &= \frac{1}{2\pi i} \int_{\mathcal{C}} K(z) \sum_{j=\max(1, n-n_0+1)}^n \left(\prod_{l=j+1}^n (\mathbf{R}(\tau_l z) \mathbf{e}_s^\top) \right) (\tau_j \mathbf{A} (\mathbf{I} - \tau_j z \mathbf{A})^{-1} \mathbf{f}_j) dz \\ &:= \frac{1}{2\pi i} \int_{\mathcal{C}} K(z) \mathbf{Q}_n^{loc}(z) dz, \end{aligned} \quad (69)$$

where

$$\mathbf{Q}_n^{loc}(z) = \mathbf{R}(\tau_n z) \mathbf{e}_s^\top \mathbf{Q}_{n-1}^{loc}(z) + \tau_n \mathbf{A} (\mathbf{I} - \tau_n z \mathbf{A})^{-1} \mathbf{f}_n, \quad \mathbf{Q}_{(n-n_0)+}^{loc}(z) = \mathbf{0}. \quad (70)$$

To approximate the local term, we select \mathcal{C} as a circle in the right half of the complex plane, enclosing the poles of the integrand, and parameterized by using elliptic functions. The same idea appears in [14] for Euler based gCQ, but we introduce the adjustments in \mathcal{C} indicated for Runge–Kutta methods in [23]. The radius of \mathcal{C} is then given by

$$M^{loc} = 5 \max \{ \|\text{spec} \mathbf{A}^{-1}\| \} / \min_{\max(1, n-n_0+1) \leq j \leq \max(n, n_0)} \{\tau_j\},$$

and centered at $M + m/10$, where

$$m^{loc} = \min \{ \text{Re}(\text{spec}(\mathbf{A}^{-1})) \} / \max_{\max(1, n-n_0+1) \leq j \leq \max(n, n_0)} \{\tau_j\}.$$

Subsequently, the quadrature rule for the local term can be formulated as follows

$$\mathbf{S}_n^{loc} \approx \sum_{l=1}^{N_Q^{loc}} w_l z_l^{-\alpha} \mathbf{Q}_n^{loc}(z_l). \quad (71)$$

We notice that the circle \mathcal{C} is fixed for the first n_0 steps, until we compute \mathbf{U}_{n_0} , and then it changes at every time step $n > n_0$.

For the history part in (68) we notice that

$$\begin{aligned} \mathbf{S}_n^{his} &= \int_0^\infty G(x) \sum_{j=1}^{n-n_0} \left(\prod_{l=j+1}^n (\mathbf{R}(-\tau_l x) \mathbf{e}_s^\top) \right) (\tau_j \mathbf{A} (\mathbf{I} + \tau_j x \mathbf{A})^{-1} \mathbf{f}_j) dx \\ &:= \int_0^\infty G(x) \left(\prod_{l=n-n_0+1}^n (\mathbf{R}(-\tau_l x) \mathbf{e}_s^\top) \right) \mathbf{Q}_{n-n_0}^{his}(x) dx, \end{aligned} \quad (72)$$

where

$$\mathbf{Q}_{n-n_0}^{his}(x) = \sum_{j=1}^{n-n_0} \left(\prod_{l=j+1}^{n-n_0} \left(\mathbf{R}(-\tau_l x) \mathbf{e}_s^\top \right) \right) (\tau_j \mathbf{A} (\mathbf{I} + \tau_j x \mathbf{A})^{-1} \mathbf{f}_j),$$

satisfying

$$\mathbf{Q}_{n-n_0}^{his}(x) = \mathbf{R}(-\tau_{n-n_0} x) \mathbf{e}_s^\top \mathbf{Q}_{n-n_0-1}^{his}(x) + \tau_{n-n_0} \mathbf{A} (\mathbf{I} + \tau_{n-n_0} \mathbf{A} x)^{-1} \mathbf{f}_{n-n_0}, \quad \mathbf{Q}_0^{his}(x) = \mathbf{0}. \quad (73)$$

In Section 6, different quadrature rules are employed depending on the form of $G(x)$. When $G(x)$ takes the form (7), the quadrature nodes x_l and weights ϖ_l are computed by using the oblivious Gauss quadrature method proposed in [4, 14]. For other types of kernels, the trapezoidal rule is used instead, see Example 2. A more optimized quadrature for each specific kernel might be arranged, but we do not pursue this issue in the present paper. In any case, this yields an approximation of the form

$$\mathbf{s}_n^{his} \approx \sum_{l=1}^{N_Q^{his}} \varpi_l G(x_l) \left(\prod_{j=n-n_0+1}^n \left(\mathbf{R}(-\tau_j x_l) \mathbf{e}_s^\top \right) \right) \mathbf{Q}_{n-n_0}^{his}(x_l). \quad (74)$$

Thus, we obtain the approximation

$$[K(\partial_t^\Delta) \mathbf{f}]_n \approx \sum_{l=1}^{N_Q^{loc}} w_l K(z_l) \mathbf{Q}_n^{loc}(z_l) + \sum_{l=1}^{N_Q^{his}} \varpi_l G(x_l) \left(\prod_{j=n-n_0+1}^n \left(\mathbf{R}(-\tau_j x_l) \mathbf{e}_s^\top \right) \right) \mathbf{Q}_{n-n_0}^{his}(x_l). \quad (75)$$

In our numerical experiments, we set

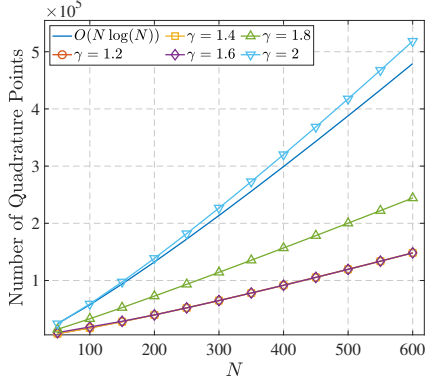
$$n_0 = \min(5, N).$$

Applying the formula from [22, Corollary 16], we choose

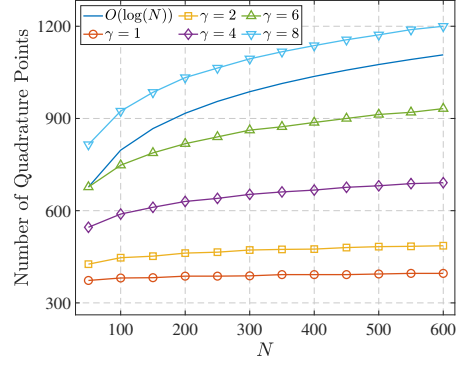
$$N_Q^{loc} = \left\lceil n_0^{\max\{1, \frac{1}{2} \log(M_{loc}) / \log(m_{loc})\}} \log(n_0) (\log(n_0) + \log(1/\text{tol})) \right\rceil \quad (76)$$

in the quadrature rule (71), where tol denotes the prescribed tolerance for the quadrature used in both (71) and (74). The total computational cost of the algorithm is $O(n_0 N_Q^{loc} + (N - n_0) N_Q^{his})$, while the memory requirement is $O(N_Q^{loc} + N_Q^{his})$. In Figure 1 we compare the total number of quadrature nodes required to approximate the fractional integral in Example 1 on graded meshes, by using the algorithm in [23] and by using the fast and oblivious algorithm in this Section. As shown, the algorithm in this Section significantly improves both efficiency and memory usage compared to the original gCQ implementation in [22]. Specifically, the total number of quadrature nodes, this is $N_Q^{loc} + N_Q^{his}$, required by our fast algorithm grows like $O(\log N)$ on the graded mesh (14), implying an overall computational complexity of $O(N \log N)$ and a memory usage of $O(\log N)$. This growth turns out to be due only to the evaluation of the history term \mathbf{s}_n^{his} , since in all the cases depicted in Figure 1 we keep fixed $N_Q^{loc} = 273$, which guarantees the high tolerance requirement $\text{tol} = 10^{-14}$ in (76).

We emphasize that thanks to the improvements in this Section we are able to choose very strongly graded meshes, with grading exponent γ up to 20. For the original implementation of the gCQ method in [22, 23], the complexity starts to become unaffordable in practice for $\gamma > 2$.



(a) Reference implementation using the quadrature rule from [22].



(b) Fast implementation introduced in Section 5.1.

Fig. 1. Comparison of the total number of quadrature points used in the gCQ scheme (68) for Example 1 on the graded mesh (14) with $\alpha = 0.5$ and $\text{tol} = 10^{-14}$.

5.2 Algorithm for the linear subdiffusion equation

This subsection presents the adaptation of the algorithm developed in Section 5.1 to discretize the linear subdiffusion equation.

$$\begin{aligned} \partial_t^\alpha v(t) + \mathcal{A}v(t) &= f(t) - \mathcal{A}u_0, \quad t \in (0, T], \\ v(0) &= 0, \end{aligned} \quad (77)$$

where $0 < \alpha < 1$, \mathcal{A} denotes an elliptic operator and u_0 is given. Define

$$\mathbf{V}(t_n) = (v(t_{n-1} + c_i \tau_n))_{i=1}^s, \quad \mathbf{V}_n = (V_{ni})_{i=1}^s,$$

with V_{ni} approximating $v(t_{n-1} + c_i \tau_n)$. To apply the fast gCQ algorithm for the fractional derivative, we observe that, by definition,

$$\partial_t^\alpha = \partial_t^{\alpha-1} \partial_t, \quad 0 < \alpha < 1.$$

Then, according to the discrete composition rule, it also holds that

$$(\partial_t^\Delta)^\alpha = (\partial_t^\Delta)^{\alpha-1} \partial_t^\Delta,$$

where ∂_t^Δ denotes the approximation of the first order derivative provided by the gCQ method, this is, [23, (29)]

$$[\partial_t^\Delta \mathbf{V}]_n = (\tau_n \mathbf{A})^{-1} (\mathbf{V}_n - v_{n-1} \mathbb{1}), \quad 1 \leq n \leq N. \quad (78)$$

Thus, we can write

$$\sum_{j=1}^n \mathbf{W}_{n,j} [\partial_t^\Delta \mathbf{V}]_j + \mathcal{A} \mathbf{V}_n = \mathbf{f}(t_n) - \mathcal{A} u_0 \mathbb{1}, \quad n \geq 1,$$

with $\mathbf{W}_{n,j}$ are gCQ weights (23) for the fractional integral operator $\partial_t^{\alpha-1}$, this is with

$$G(x) = \frac{\sin(\pi(1-\alpha))}{\pi} x^{\alpha-1}.$$

Subsequently, we have

$$\mathbf{W}_{n,n} [\partial_t^\Delta \mathbf{V}]_n + \mathcal{A} \mathbf{V}_n = \mathbf{f}(t_n) - \mathcal{A} u_0 - \sum_{j=1}^{n-1} \mathbf{W}_{n,j} [\partial_t^\Delta \mathbf{V}]_j, \quad n \geq 1.$$

Noting from (25) that $\mathbf{W}_{n,n} = (\tau_n \mathbf{A})^{1-\alpha}$, and combining this with (78), the numerical scheme can be reformulated as

$$((\tau_n \mathbf{A})^{-\alpha} I + \mathcal{A}) \mathbf{V}_n = \mathbf{f}(t_n) - \mathcal{A} \mathbf{U}_0 + (\tau_n \mathbf{A})^{-\alpha} v_{n-1} \mathbb{1} - \sum_{j=1}^{n-1} \mathbf{W}_{n,j} [\partial_t^\Delta \mathbf{V}]_j, \quad n \geq 1. \quad (79)$$

The efficient evaluation of the right-hand side summation term employs the algorithm from Section 5.1 by splitting it into two parts

$$\sum_{j=1}^{n-1} \mathbf{W}_{n,j} [\partial_t^\Delta \mathbf{V}]_j = \sum_{j=1}^{n-n_0} \mathbf{W}_{n,j} [\partial_t^\Delta \mathbf{V}]_j + \sum_{j=\max(1, n-n_0+1)}^{n-1} \mathbf{W}_{n,j} [\partial_t^\Delta \mathbf{V}]_j. \quad (80)$$

The history part is approximated via

$$\sum_{j=1}^{n-n_0} \mathbf{W}_{n,j} [\partial_t^\Delta \mathbf{V}]_j \approx \sum_{l=1}^{N_Q^{his}} \varpi_l G(x_l) \left(\prod_{j=n-n_0+1}^n \left(\mathbf{R}(-\tau_j x_l) \mathbf{e}_s^\top \right) \right) \mathbf{Q}_{n-n_0}^{his}(x_l),$$

where $\mathbf{Q}_{n-n_0}^{his}$ is defined as in (73), with \mathbf{f}_j taken to be $[\partial_t^\Delta \mathbf{V}]_j$. For the local part, the approximation is given by

$$\sum_{j=\max(1, n-n_0+1)}^{n-1} \mathbf{W}_{n,j} [\partial_t^\Delta \mathbf{V}]_j \approx \sum_{l=1}^{N_Q^{loc}} w_l z_l^{\alpha-1} \mathbf{R}(\tau_n z_l) \mathbf{e}_s^\top \mathbf{Q}_{n-1}^{loc}(z_l),$$

where \mathbf{Q}_{n-1}^{loc} satisfies (70), with \mathbf{f}_{n-1} replaced by $[\partial_t^\Delta \mathbf{V}]_{n-1}$.

6 Numerical experiments

In this section, we consider the application of Runge–Kutta based gCQ to compute convolution integrals, solve fractional diffusion equations, and nonlinear wave equations with damping terms of convolution type, in order to test the algorithm in Section 5.1 and verify the theoretical findings presented in Theorems 5. The solutions of the problems under consideration exhibit nonsmooth behavior near the origin and in some cases also at times away from the origin. In all cases, the approximation on uniform time meshes suffers from some sort of order reduction. To achieve full-order convergence, we have implemented the Runge–Kutta based gCQ scheme on graded meshes with a quadrature tolerance $\text{tol} = 10^{-14}$ for the fast and oblivious algorithm. When possible, the grading parameter is selected according to Theorem 5 and, in the case of Example 5, which is not fully covered by our theory, heuristically. Notice that in this last example we deal with a nonlinear wave problem and error analysis techniques based uniquely on the preservation of the composition rule by the gCQ method are not enough to justify the observed high order of convergence, cf. [1].

6.1 Computation of convolution with different kernels

Example 1. Consider the Runge–Kutta based gCQ approximation (75) for the fractional integral

$$\partial_t^{-\alpha} f(t) = \int_0^t \frac{(t-s)^{\alpha-1}}{\Gamma(\alpha)} f(s) ds, \quad (81)$$

with $f(t) = t^\beta$ and the exact solution is then given by

$$\partial_t^{-\alpha} t^\beta = \frac{\Gamma(\beta+1)}{\Gamma(\alpha+\beta+1)} t^{\alpha+\beta}. \quad (82)$$

Set $T = 1$. The maximum absolute error in the numerical results is measured by

$$\max_{1 \leq n \leq N} \left| [\partial_t^{-\alpha} f](t_n) - [(\partial_t^\Delta)^{-\alpha} f]_n \right|. \quad (83)$$

By applying the two-stage Radau IIA based gCQ scheme and selecting different values for α and β , we illustrate the maximum absolute error on the graded mesh (14) with $\gamma = 3/(\alpha + \beta)$ in Figure 2. The results demonstrate third-order convergence, which aligns with the theoretical findings in Theorem 5.

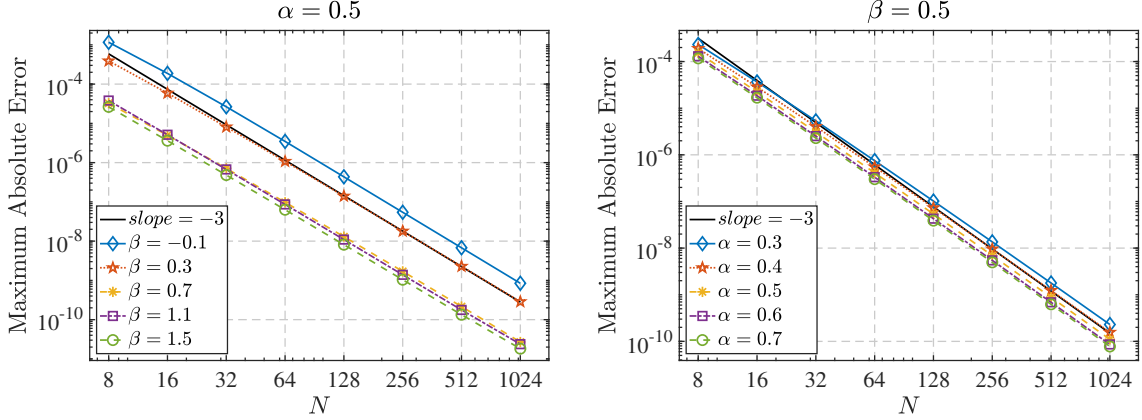


Fig. 2. Maximum absolute error of the two-stage Radau IIA scheme for Example 1 on (14) with $\gamma = \frac{3}{\alpha + \beta}$.

Example 2. Consider the Runge–Kutta based gCQ approximation (75) for convolutions (1) with the following two kernels:

$$k_a(t) = -\frac{d}{dt} E_{\alpha,1}(-t^\alpha), \quad k_b(t) = \frac{t^{\alpha-1}}{\Gamma(\alpha)} e^{-t}, \quad (84)$$

acting on the function

$$f(t) = t^\beta.$$

The Laplace transforms of the kernels in (84) are given by

$$K_a(z) = \frac{1}{z^\alpha + 1}, \quad K_b(z) = \frac{1}{(z + 1)^\alpha},$$

both satisfy Assumption 1. The gCQ approximations take the form

$$[K_a(\partial_t^\Delta) f]_n = \int_0^\infty G_a(x) y_n^a(x) dx, \quad [K_b(\partial_t^\Delta) f]_n = \int_0^\infty G_b(x) y_n^b(x) dx,$$

where

$$G_a(x) = \frac{\sin(\pi\alpha)}{\pi} \frac{x^\alpha}{x^{2\alpha} + 2x^\alpha \cos(\pi\alpha) + 1}, \quad G_b(x) = \frac{\sin(\pi\alpha)}{\pi} x^{-\alpha}, \quad 0 < \alpha < 1,$$

and

$$y_n^a(x) = y_n(x), \quad y_n^b(x) = y_n(x + 1),$$

with $y_n(x)$ given in (20).

Notice that the function G_a does not fit the behavior for which the quadrature in [4] was designed. Thus, we use trapezoidal quadrature to evaluate the history part of the

convolution $[K_a(\partial_t^\Delta)f]_n$. Notice that the substitution $x = e^{\mu/\alpha}$ transforms the integral (72), with $G(x) = G_a(x)$, into

$$\mathbf{S}_n^{\text{his}} = \frac{1}{\alpha} \int_{-\infty}^{\infty} e^{\mu/\alpha} G_a(e^{\mu/\alpha}) \left(\prod_{l=n-n_0+1}^n \left(\mathbf{R}(-\tau_l e^{\mu/\alpha}) \mathbf{e}_s^\top \right) \right) \mathbf{Q}_{n-n_0}^{\text{his}}(e^{\mu/\alpha}) d\mu.$$

Applying the trapezoidal rule yields the approximation

$$\mathbf{S}_n^{\text{his}} \approx \frac{h}{\alpha} \sum_{l=-\tilde{M}}^{\tilde{N}} e^{lh/\alpha} G_a(e^{lh/\alpha}) \left(\prod_{l=n-n_0+1}^n \left(\mathbf{R}(-\tau_l e^{lh/\alpha}) \mathbf{e}_s^\top \right) \right) \mathbf{Q}_{n-n_0}^{\text{his}}(e^{lh/\alpha}),$$

where the quadrature parameters $h = 3/40$ and $\tilde{M} = \tilde{N} = 400$ are chosen to ensure that the quadrature error is negligible. The maximum absolute error for $K(z) = K_a(z)$ is computed in the same manner as in (83). The exact solution is given by

$$(K_a(\partial_t)f)(t) = \Gamma(\beta + 1)t^{\alpha+\beta} E_{\alpha, \alpha+\beta+1}(-t^\alpha),$$

with the Mittag-Leffler function evaluated using the routine from [11].

The results in Figure 3a show that the two-stage Radau IIA based gCQ method achieves a full convergence order of 3 on the graded mesh (14) with $\gamma = 3/(\alpha + \beta)$. In Figure 3b, it is evident that the convergence rate on the graded mesh is $\min\{3, \gamma(\alpha + \beta)\}$. Additionally, Figure 4 presents the case of $p > q + 1 + \alpha$, verifying that the Runge–Kutta based gCQ method can attain a convergence order of $\min\{p, q + 1 + \alpha\}$ and maintain this rate for nonsmooth $f(t)$ on a graded mesh (14) with $\gamma = \min\{p, q + 1 + \alpha\}/(\alpha + \beta)$. These results are consistent with Theorems 4 and 5.

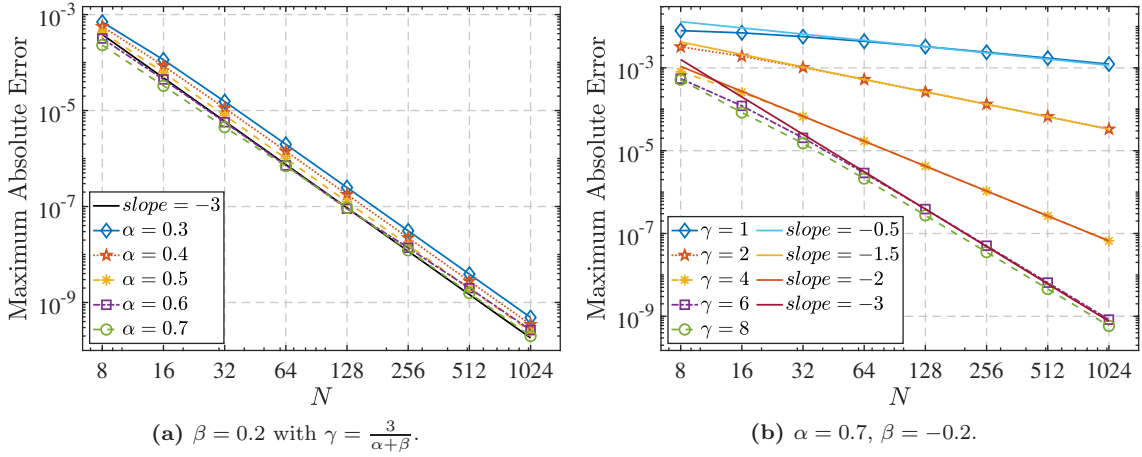


Fig. 3. Maximum absolute error of the two-stage Radau IIA scheme for Example 2 with $k = k_a$.

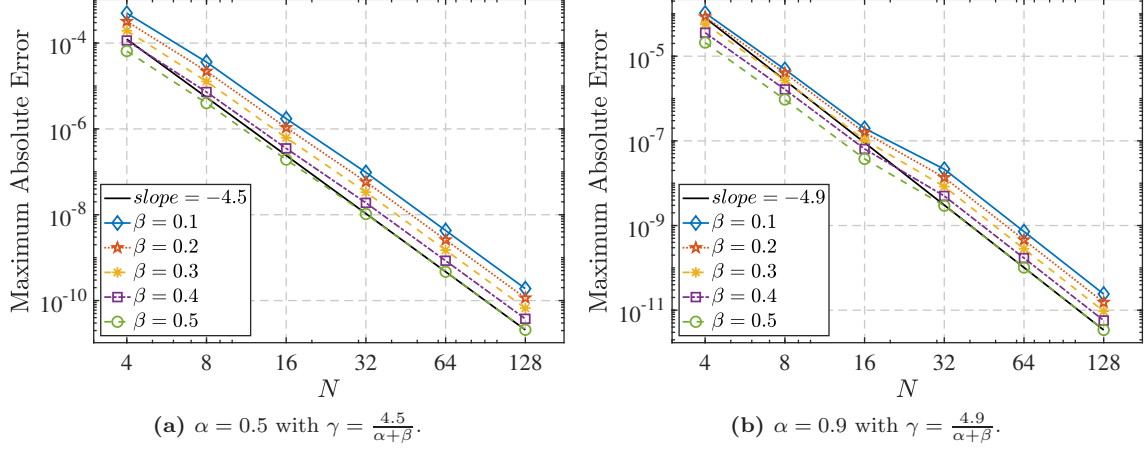


Fig. 4. Maximum absolute error of the four-stage Lobatto IIIC scheme for Example 2 with $k = k_a$.

Denote u_n^{ref} as the numerical solution $[K_b(\partial_t^\Delta)f]_n$ computed on a finer graded time mesh

$$t_n = \left(\frac{n}{2N}\right)^\gamma, \quad 1 \leq n \leq 2N, \quad (85)$$

the maximum absolute error in Figure 5 is computed by

$$\max_{1 \leq n \leq N} |u_n^{\text{ref}} - [K_b(\partial_t^\Delta)f]_n|.$$

The results in Figure 5 show that the fast algorithm for computing $[K_b(\partial_t^\Delta)f]_n$ works well on the strongly graded mesh and the obtained convergence rate on the graded mesh agrees with the results in Theorem 5.

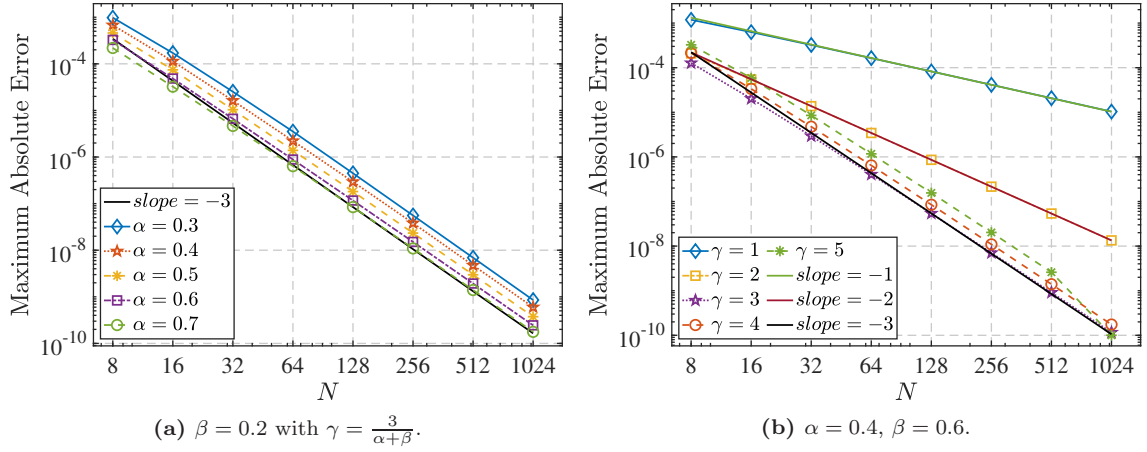


Fig. 5. Maximum absolute error of the two-stage Radau IIA scheme for Example 2 with $k = k_b$.

6.2 Differential equations

Example 3. We consider the fractional ordinary diffusion equation

$$D_t^\alpha u(t) + u(t) = f(t), \quad u(0) = 1, \quad 0 < t \leq 1,$$

with the exact solution

$$u(t) = 1 + t^{\beta_1} + H(t - \sigma)(t - \sigma)^{\beta_2}, \quad t \geq 0,$$

where $\beta_1 > -1$, $\beta_2 > \alpha$, and $H(\cdot)$ denotes the Heaviside function. The corresponding source term takes the form

$$f(t) = u(t) + \frac{\Gamma(\beta_1 + 1)}{\Gamma(\beta_1 - \alpha + 1)} t^{\beta_1 - \alpha} + \frac{\Gamma(\beta_2 + 1)}{\Gamma(\beta_2 - \alpha + 1)} H(t - \sigma)(t - \sigma)^{\beta_2 - \alpha},$$

exhibiting piecewise smooth behavior.

For this example, we employ a graded mesh with higher density near the singularities $t = 0$ and $t = \sigma$, defined as

$$\begin{aligned} N_1 &= \lfloor N\sigma/T \rfloor, \quad \mathbf{l}(n) = n^{\gamma_1 - 1} (N_1 - n + 1)^{\gamma_2 - 1} N_1^{-\gamma_1 - \gamma_2 + 1}, \quad 1 \leq n \leq N_1, \\ t(0) &= 0, \quad t(n) = t(n-1) + \tau(n), \quad \tau(n) = \frac{\sigma}{\|\mathbf{l}\|_{l^1}} \mathbf{l}(n), \quad 1 \leq n \leq N_1, \\ t(k) &= t(N_1) + (T - \sigma) \left(\frac{k - N_1}{N - N_1} \right)^{\gamma_2}, \quad N_1 + 1 \leq k \leq N - 1, \quad t(N) = T. \end{aligned} \quad (86)$$

In Figure 6a, the structure of the mesh defined in (86) is illustrated, showing that the time step size near $t = 0$ and $t = \sigma$ is of order $O(N^{-\gamma_1})$ and $O(N^{-\gamma_2})$, respectively, while the maximum step size is of order $O(N^{-1})$. The numerical solution, displayed in Figure 6b, accurately captures the exact solution behavior, even at the discontinuity point $t = \sigma$. Moreover, as confirmed in Figure 7, the optimal convergence order $\min\{p, q + 1 + \alpha\}$ is asymptotically attained by choosing $\gamma_1 = \min\{p, q + 1 + \alpha\}/\beta_1$ and $\gamma_2 = \min\{p, q + 1 + \alpha\}/\beta_2$.

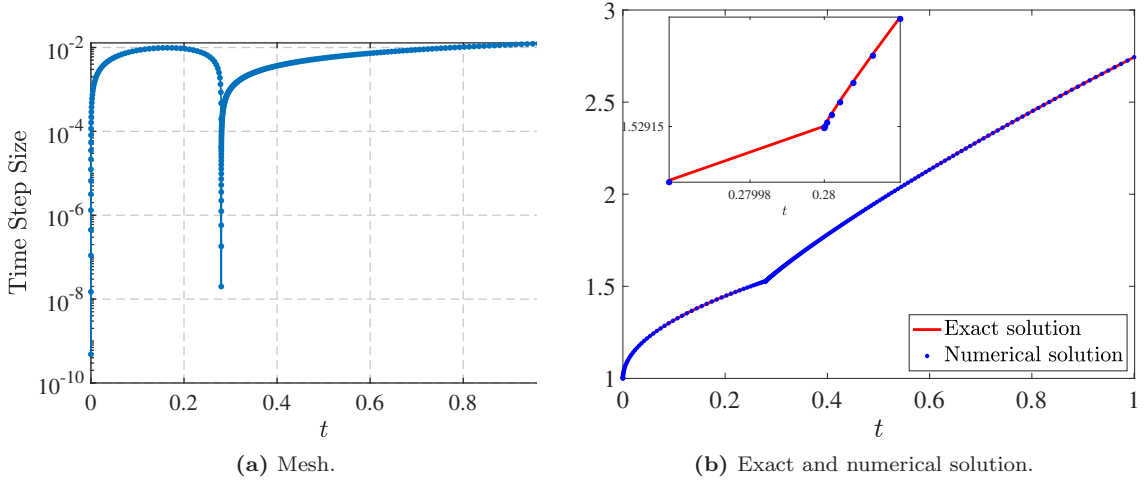


Fig. 6. The structure of mesh (86) and two-stage Radau IIA based gCQ solution with $N = 256$, $\sigma = 0.28$, $\beta_1 = 0.5$, $\beta_2 = 0.9$, $\gamma_1 = 3/\beta_1$, $\gamma_2 = 3/\beta_2$.

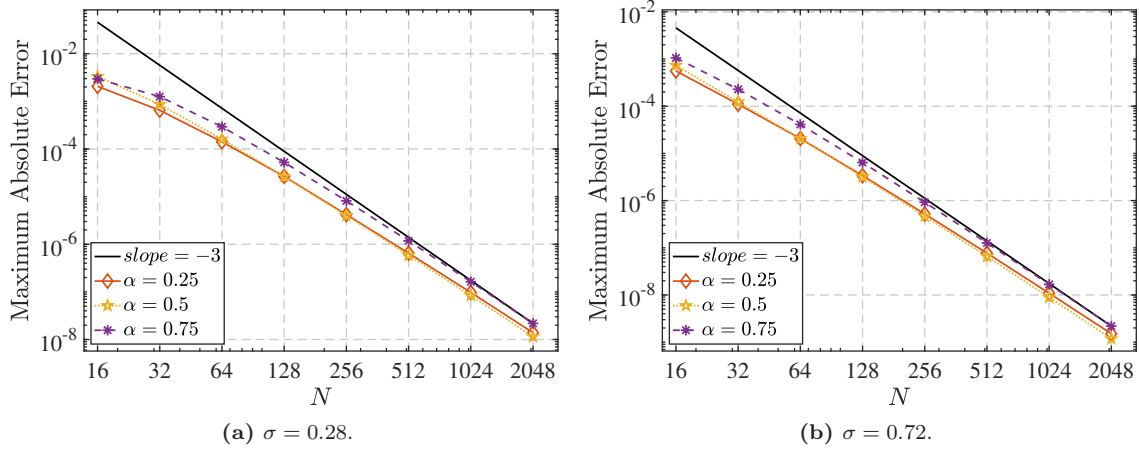


Fig. 7. Maximum absolute error using the two-stage Radau IIA for Example 3 with $\beta_1 = 0.5$, $\beta_2 = 0.9$, $\gamma_1 = 3/\beta_1$, $\gamma_2 = 3/\beta_2$.

Example 4. In this example, we consider the approximation of the two dimensional partial differential equations

$$\partial_t^\alpha u - u_{xx} - u_{yy} = f,$$

with initial conditions

$$u(x, y, 0) = 0, \quad (x, y) \in \Omega,$$

and boundary conditions

$$u(x, y, t) = 0, \quad (x, y) \in \partial\Omega, \quad 0 < t \leq 1.$$

The exact solution is given by

$$u(x, y, t) = t^\alpha \cos\left(\frac{\pi}{2}x\right) \cos\left(\frac{\pi}{2}y\right),$$

and the source term is

$$f(x, y, t) = \left(\Gamma(\alpha + 1) + \frac{\pi^2}{2}t^\alpha\right) \cos\left(\frac{\pi}{2}x\right) \cos\left(\frac{\pi}{2}y\right).$$

In our numerical experiments, we consider the domain $\Omega = (-1, 1)^2$ and employ a fourth-order compact finite difference scheme [35] with uniform grid spacing $\Delta_x = \Delta_y = \frac{1}{128}$ for spatial discretization. In Figures 8 and 9, we compare the two-stage Radau IIA based gCQ method with the corrected third-order backward differentiation method from [16]. These results show that for solutions with limited temporal regularity, the full convergence order is not preserved when using the corrected scheme in [16], whereas the Runge–Kutta based gCQ method on graded meshes recovers optimal convergence both at the final time point and across all evaluated time steps. Notice that the optimal grading parameter in this case is $\gamma = \frac{3}{\alpha}$, which corresponds to the case $\beta = 0$, $p = 3$, $q = 2$, in Theorem 5. According to the analysis in [14, Section 4], the optimal time mesh is determined by the behaviour of the source term f close to 0, rather than the behaviour of the exact solution u , and the numerical experiments confirm the theory.

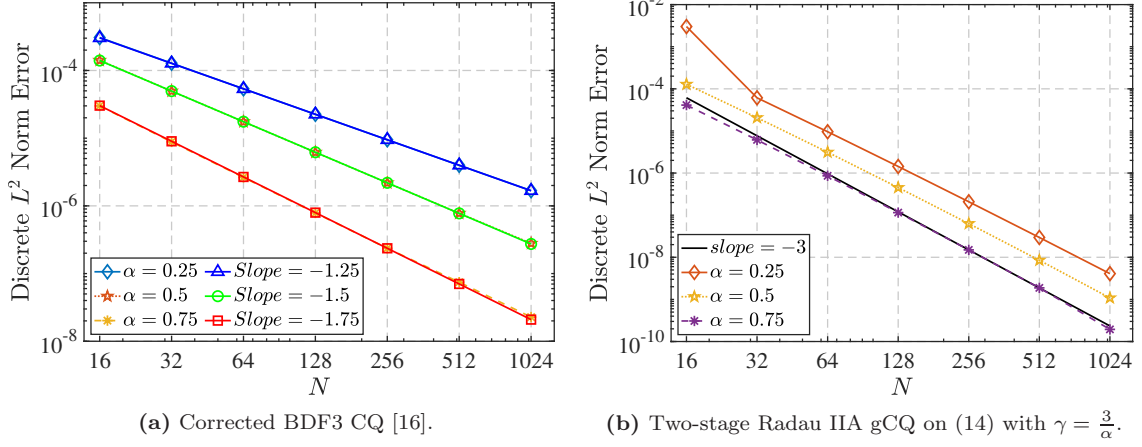


Fig. 8. Comparisons of discrete L^2 norm errors for Example 4 at the final time $t_N = 1$.

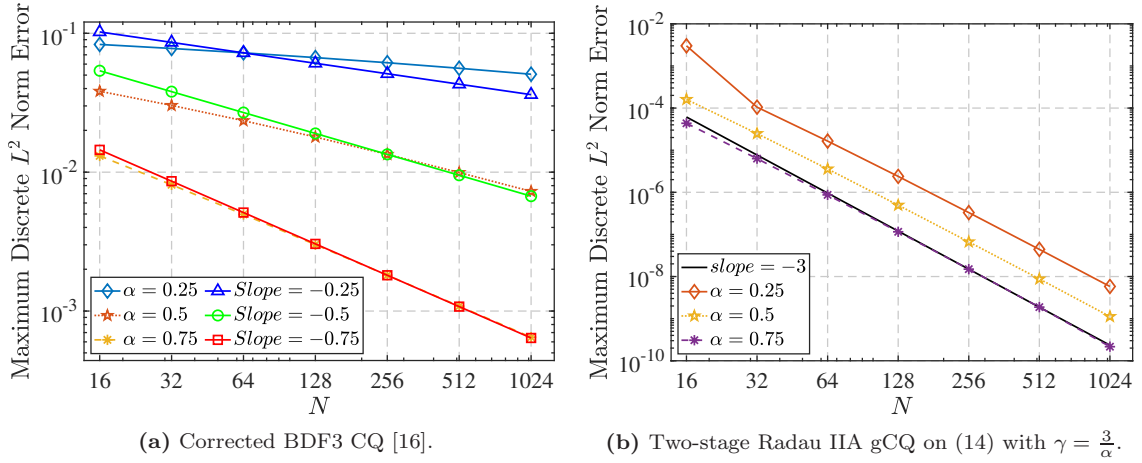


Fig. 9. Comparisons of maximum discrete L^2 norm errors for Example 4.

Example 5. Consider the following Westervelt equation [1]

$$\begin{cases} (1 - 2\kappa u)\partial_t^2 u - u_{xx} - k * \partial_t u_{xx} = 2\kappa(\partial_t u)^2 + f, & x \in (-8, 8), \quad t \in (0, 2], \\ u(0, t) = u(1, t) = 0, & t \in (0, 2], \\ u(x, 0) = \frac{e^{-x^2}}{2}, \quad \partial_t u(x, 0) = 0, & x \in (-8, 8), \end{cases} \quad (87)$$

where

$$k(t) = \frac{t^{\alpha-1}}{\Gamma(\alpha)} e^{-t}, \quad f(x, t) = (1 + \log(t)) \sin(\pi x), \quad t \in (0, 2], \quad x \in (-8, 8).$$

Applying the Runge–Kutta based gCQ method for temporal discretization and the fourth-order compact difference scheme [35] for spatial discretization with J uniform grid subdivisions, the fully discrete scheme for solving (87) is given by

$$\begin{cases} (1 - 2\kappa \mathbf{U}_n^h) [(\partial_t^\Delta)^2 \mathbf{U}^h]_n - \mathbf{L} \mathbf{U}_n^h - [K(\partial_t^\Delta) (\partial_t^\Delta \mathbf{L} \mathbf{U}^h)]_n = 2\kappa [\partial_t^\Delta \mathbf{U}^h]_n^2, \\ \mathbf{U}_0^h = \mathbf{0}, \quad \partial_t^\Delta \mathbf{U}_0^h = (\sin(\pi x_j))_{j=1}^{J-1}, \quad x_j = 2j/J, \quad 1 \leq j \leq J-1. \end{cases} \quad (88)$$

Here, the matrix \mathbf{L} is derived by applying the compact difference method [35] to approximate u_{xx} . The operator ∂_t^Δ is defined in (78). The term $[(\partial_t^\Delta)^2 \mathbf{U}^h]_n$ is obtained by

applying ∂_t^Δ to $[\partial_t^\Delta \mathbf{U}^h]_n$, which is given by

$$[(\partial_t^\Delta)^2 \mathbf{U}^h]_n = (\tau_n \mathbf{A})^{-1} \left([\partial_t^\Delta \mathbf{U}^h]_n - \mathbf{e}_s^\top [\partial_t^\Delta \mathbf{U}^h]_{n-1} \mathbb{1} \right).$$

In the implementation, the fast algorithm shown in Section 5 is employed to approximate $[K(\partial_t^\Delta)(\partial_t^\Delta \mathbf{L} \mathbf{U}^h)]_n$, and the nonlinear system (88) is solved by the fixed point iteration with a tolerance of 10^{-8} . With spatial mesh size $h = 1/16$, the maximum discrete L^2 norm error is measured by

$$\max_{1 \leq n \leq N} \|\tilde{u}_{2n}^h - u_n^h\|_h,$$

where

$$\|v\|_h^2 = h \sum_{j=1}^{J-1} (v^j)^2$$

denotes the discrete L^2 norm, and \tilde{u}_{2n}^h represents the numerical solution computed on the refined time mesh (85).

From the numerical results in Figures 10 and 11, we observe that employing a graded mesh (14) with $\gamma = 3$ yields full third-order convergence asymptotically. In contrast, when using the uniform mesh, that is, (14) with $\gamma = 1$, the convergence rate is limited to first order. The evolution of the numerical solution is shown in Figure 12. It can be observed that the case with $\kappa = 0.09$ attains slightly larger solution values at the final time $T = 2$ on the domain $(-8, 8)$. Moreover, the temporal evolution of the numerical solution indicates that the maximum values in the x -direction for both $\kappa = 0$ and $\kappa = 0.09$ exhibit the same qualitative behavior: decreasing over the time interval $(0, 1]$ and increasing thereafter. Figure 13 further demonstrates that the Runge–Kutta based gCQ method, when implemented on the graded mesh (14) with $\gamma = 3$, yields reduced maximum errors near the final time compared to those obtained using a uniform mesh. It turns out that increasing the accuracy near the origin improves globally the error, even if its maximum is attained at the final time of integration $T = 2$, see Figure 13. These results demonstrate the effectiveness of the Runge–Kutta based gCQ method in solving equations involving convolution integrals.

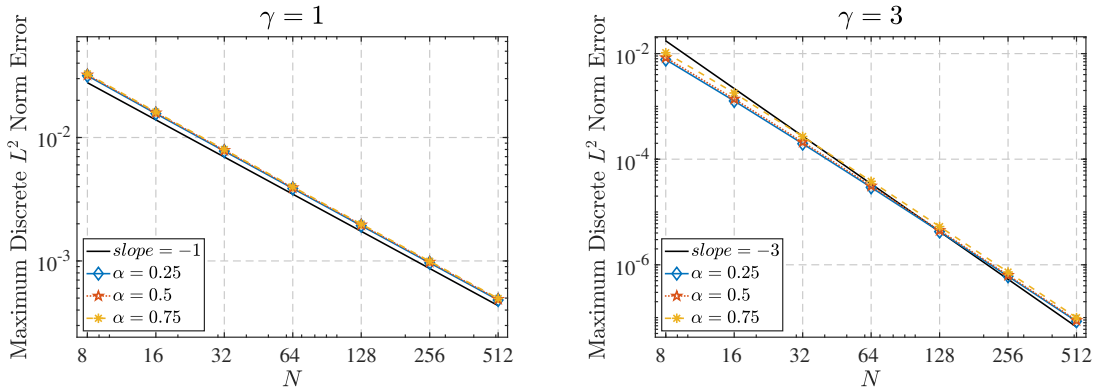


Fig. 10. Maximum discrete L^2 norm errors of the two-stage Radau IIA Runge–Kutta based gCQ method for Example 5 with $\kappa = 0$.

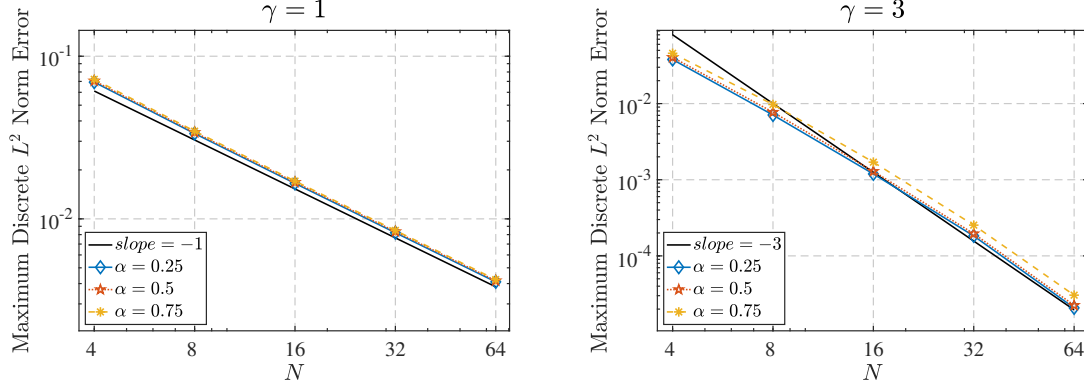


Fig. 11. Maximum discrete L^2 norm errors of the two-stage Radau IIA Runge-Kutta based gCQ method for Example 5 with $\kappa = 0.09$.

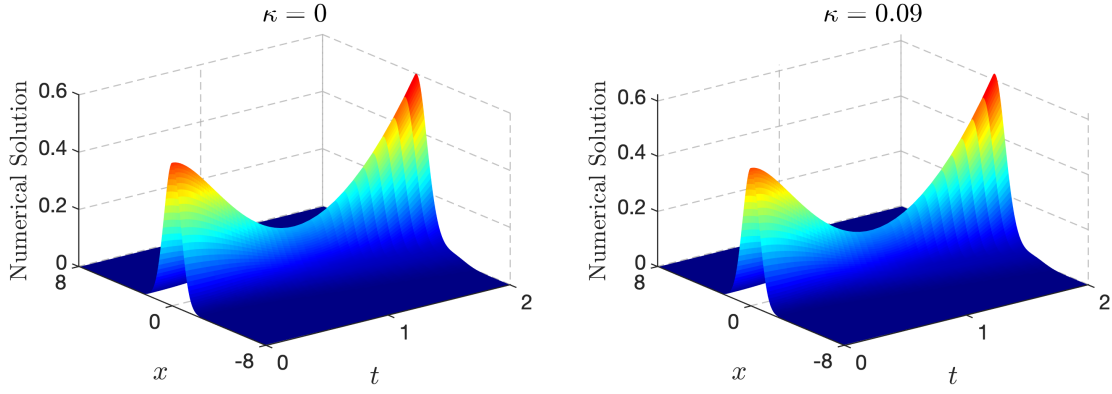


Fig. 12. Numerical solution of the two-stage Radau IIA Runge-Kutta based gCQ method for Example 5 with $\alpha = 0.5$, $\gamma = 3$ and $N = 64$.

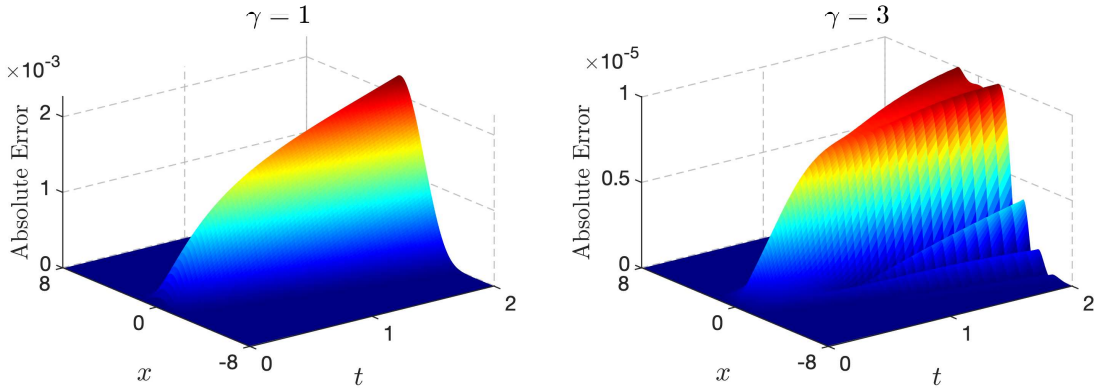


Fig. 13. Absolute error of the two-stage Radau IIA Runge-Kutta based gCQ method for Example 5 with $\alpha = 0.5$, $\kappa = 0.09$ and $N = 64$.

Acknowledgements

The second author has been supported by “Proyecto 16 - proyecto G Plan Propio” of the University of Malaga and by grant PID2022-137637NB-C21 funded by MICI-U/AEI/10.13039/501100011033 and ERDF/EU.

Data availability statement

The codes implementing the algorithms discussed in this article are publicly available at: <https://github.com/jingguo-math/gCQrK>. No other data are associated with the manuscript.

A Identities

This appendix collects essential mathematical results used in our analysis. We begin with the definition of the Mittag-Leffler function, followed by key identities and estimates for solutions to (11). The proofs of these results follow the techniques in [14, Lemma 6].

Definition 24. [Mittag-Leffler function] For $\alpha > 0$, $\beta \in \mathbb{R}$, the two parameter Mittag-Leffler function $E_{\alpha,\beta}(z)$ is defined by

$$E_{\alpha,\beta}(z) = \sum_{\ell=0}^{\infty} \frac{z^{\ell}}{\Gamma(\alpha\ell + \beta)}, \quad z \in \mathbb{C}.$$

Lemma 25. For $\beta > -1$, $m \in \mathbb{N}$, it holds

1. For $0 < \alpha < 1$, $\zeta > 0$, we have

$$\int_0^{\infty} x^{-\alpha} \frac{1}{1 + \zeta x} dx = B(\alpha, 1 - \alpha) \zeta^{\alpha-1}, \quad (89)$$

where B is the Beta function.

2. [32, Theorem 1.6] For $\alpha < 2$, $\beta \in \mathbb{R}$, there exists a constant $C > 0$ such that

$$|E_{\alpha,\beta}(-x)| \leq \frac{C}{1 + x}, \quad x \geq 0.$$

3. The solution to (11) with $f(t) = t^{\beta} \mathbf{v}$ is

$$y(x, t) = \Gamma(\beta + 1) \sum_{\ell=0}^{\infty} \frac{(-x)^{\ell}}{\ell!} \frac{\Gamma(\ell + 1)}{\Gamma(\ell + \beta + 2)} t^{\ell+\beta+1} \mathbf{v}, \quad \forall \beta > -1.$$

Especially, for $\beta \in \mathbb{N}$, it can be rewritten as

$$y(x, t) = \beta! (-x)^{-(\beta+1)} \left(e^{-xt} - \sum_{\ell=0}^{\beta} \frac{(-xt)^{\ell}}{\ell!} \right) \mathbf{v}.$$

4. The derivatives of the solution to (11) with $f(t) = t^{\beta} \mathbf{v}$ with $\beta > -1$ can be expressed explicitly. For $\beta \notin \mathbb{N}$, the expression is given by

$$\frac{\partial^m y}{\partial t^m}(x, t) = \Gamma(\beta + 1) t^{\beta-m+1} E_{1,\beta-m+2}(-xt) \mathbf{v},$$

while for $\beta \in \mathbb{N}$, it takes the form

$$\frac{\partial^m y}{\partial t^m}(x, t) = \begin{cases} \beta! t^{\beta-m+1} E_{1,\beta-m+2}(-xt) \mathbf{v}, & \text{if } m \leq \beta, \\ \beta! (-x)^{-\beta+m-1} e^{-xt} \mathbf{v}, & \text{if } m \geq \beta + 1. \end{cases}$$

In both cases, the derivatives satisfy

$$\left\| \frac{\partial^m y}{\partial t^m}(x, t) \right\|_{\mathcal{X}} \leq \Gamma(\beta + 1) t^{\beta-m+1} \frac{C}{1 + xt}, \quad (90)$$

where the constant C depends on $\|\mathbf{v}\|_{\mathcal{X}}$, β and m . In particular, if $\beta \in \mathbb{N}$ and $m \geq \beta + 1$, then $C = (m - \beta)! \|\mathbf{v}\|_{\mathcal{X}}$.

5. The m -th derivative of the solution to (11) with $f(t) = H(t - \eta)(t - \eta)^\beta \mathbf{v}$, where $\beta \geq 0$, $m \leq \beta + 2$, and $\eta \geq 0$, can be expressed explicitly. For $\beta \notin \mathbb{N}$, the expression is given by

$$\begin{aligned} \frac{\partial^m y}{\partial t^m}(x, t) &= \Gamma(\beta + 1)H(t - \eta)(t - \eta)^{\beta-m+1}E_{1, \beta-m+2}(-x(t - \eta))\mathbf{v} \\ &\quad + \Gamma(\beta + 1)\delta(t - \eta)(t - \eta)^{\beta-m+2}E_{1, \beta-m+3}(-xt)\mathbf{v}, \end{aligned}$$

while for $\beta \in \mathbb{N}$, it takes the form

$$\frac{\partial^m y}{\partial t^m}(x, t) = \begin{cases} \beta! H(t - \eta)(t - \eta)^{\beta-m+1}E_{1, \beta-m+2}(-x(t - \eta))\mathbf{v}, & \text{if } m \leq \beta, \\ \beta! H(t - \eta)e^{-x(t-\eta)}\mathbf{v}, & \text{if } m = \beta + 1 \\ \beta! (-H(t - \eta)xe^{-x(t-\eta)} + \delta(t)e^{-x(t-\eta)})\mathbf{v}, & \text{if } m = \beta + 2. \end{cases}$$

In both cases, the derivatives satisfy

$$\left\| \frac{\partial^m y}{\partial t^m}(x, t) \right\|_{\mathcal{X}} \leq C\Gamma(\beta + 1) \frac{H(t - \eta)(t - \eta)^{\beta-m+1} + \delta(t - \eta)(t - \eta)^{\beta-m+2}}{1 + xt}. \quad (91)$$

B Estimates on the graded mesh

Some estimates on the graded mesh defined in (14) are provided below.

Lemma 26. Let $m > 0$, and consider the time mesh defined in (14) with step sizes τ_j . Then for any $\sigma_j \in [t_{j-1}, t_j]$, $2 \leq j \leq n$, the following estimates hold

$$\tau_j^{\nu_1+m} \sigma_j^{\nu_2-m} \leq C \begin{cases} T^{\nu_1+\nu_2} N^{-\gamma(\nu_1+\nu_2)}, & \gamma(\nu_1 + \nu_2) < m, \\ T^{m/\gamma} N^{-m} t_j^{\nu_1+\nu_2-m/\gamma}, & \gamma(\nu_1 + \nu_2) \geq m, \end{cases} \quad (92)$$

and moreover,

$$\sum_{j=2}^n \tau_j^m \sigma_j^{\nu-m} \leq C \begin{cases} N^{-\gamma\nu}, & \gamma\nu < m - 1, \\ N^{-(m+1)} \log(n), & \gamma\nu = m - 1, \\ N^{-(m+1)} t_n^{\nu-(m+1)/\gamma}, & \gamma\nu > m - 1, \end{cases} \quad (93)$$

where $C > 0$ is a constant independent of the mesh.

Proof. From the graded mesh definition (14), it follows that

$$\tau_j \leq \gamma j^{\gamma-1} \tau^\gamma,$$

and

$$\sigma_j^{\nu_2-m} \leq \max\{(j-1)^{\gamma(\nu_2-m)}, j^{\gamma(\nu_2-m)}\} \tau^{\gamma(\nu_2-m)},$$

Hence,

$$\tau_j^{\nu_1+m} \sigma_j^{\nu_2-m} \leq \gamma^{\nu_1+m} j^{(\nu_1+m)(\gamma-1)} \max\{(j-1)^{\gamma(\nu_2-m)}, j^{\gamma(\nu_2-m)}\} \tau^{\gamma(\nu_1+\nu_2)}.$$

Using the inequality $j/2 \leq j-1 \leq j$ for $j \geq 2$, we obtain

$$\tau_j^{\nu_1+m} \sigma_j^{\nu_2-m} \leq \max\{1, 2^{\gamma(m-\nu_2)}\} \gamma^{\nu_1+m} j^{\gamma(\nu_1+\nu_2)-m} \tau^{\gamma(\nu_1+\nu_2)}.$$

This leads to

$$\tau_j^{\nu_1+m} \sigma_j^{\nu_2-m} \leq \max\{1, 2^{\gamma(m-\nu_2)}\} \gamma^{\nu_1+m} \begin{cases} T^{\nu_1+\nu_2} N^{-\gamma(\nu_1+\nu_2)}, & \gamma(\nu_1 + \nu_2) < m, \\ T^{m/\gamma} N^{-m} t_j^{(\nu_1+\nu_2)-m/\gamma}, & \gamma(\nu_1 + \nu_2) \geq m, \end{cases}$$

and

$$\begin{aligned} \sum_{j=2}^n \tau_j^m \sigma_j^{\nu-m} &\leq \max\{1, 2^{\gamma(m-\nu)}\} \gamma^m \tau^{\gamma\nu} \sum_{j=2}^n j^{\gamma\nu-m} \\ &\leq \max\{1, 2^{\gamma(m-\nu)}\} \gamma^m T^\nu \begin{cases} N^{-\gamma\nu}, & \gamma\nu < m-1, \\ N^{-m+1} \log(n), & \gamma\nu = m-1, \\ 2^{\gamma\nu-m+1} N^{-m+1} t_n^{\nu-(m-1)/\gamma}, & \gamma\nu > m-1. \end{cases} \end{aligned}$$

The proof is completed. \square

References

- [1] K. Baker, L. Banjai, and M. Ptashnyk. Numerical analysis of a time-stepping method for the Westervelt equation with time-fractional damping. *Math. Comp.*, 2024.
- [2] L. Banjai and M. Ferrari. Generalized convolution quadrature based on the trapezoidal rule. *arXiv preprint arXiv:2305.11134*, 2023.
- [3] L. Banjai and M. Ferrari. Runge–Kutta convolution quadrature based on Gauss methods. *Numer. Math.*, 156(5):1719–1750, 2024.
- [4] L. Banjai and M. López-Fernández. Efficient high order algorithms for fractional integrals and fractional differential equations. *Numer. Math.*, 141(2):289–317, 2019.
- [5] L. Banjai and M. López-Fernández. Numerical approximation of the Schrödinger equation with concentrated potential. *J. Comput. Phys.*, 405:109155, 21, 2020.
- [6] L. Banjai and C. Lubich. An error analysis of Runge–Kutta convolution quadrature. *BIT*, 51:483–496, 2011.
- [7] L. Banjai, C. Lubich, and J. M. Melenk. Runge–Kutta convolution quadrature for operators arising in wave propagation. *Numer. Math.*, 119(1):1–20, 2011.
- [8] L. Banjai and C. G. Makridakis. A posteriori error analysis for approximations of time-fractional subdiffusion problems. *Math. Comp.*, 91(336):1711–1737, 2022.
- [9] L. Banjai and F.-J. Sayas. *Integral Equation Methods for Evolutionary PDE: A Convolution Quadrature Approach*, volume 59. Springer Nature, 2022.
- [10] E. Cuesta, C. Lubich, and C. Palencia. Convolution quadrature time discretization of fractional diffusion-wave equations. *Math. Comp.*, 75(254):673–696, 2006.
- [11] R. Garrappa. Numerical evaluation of two and three parameter Mittag-Leffler functions. *SIAM J. Numer. Anal.*, 53(3):1350–1369, 2015.
- [12] R. Gorenflo, A. A. Kilbas, F. Mainardi, and S. Rogosin. *Mittag-Leffler functions, related topics and applications*. Springer Monographs in Mathematics. Springer, Berlin, 2020. Second edition [of 3244285].

- [13] J. Guo and M. Lopez-Fernandez. Accompanying codes published at github. <https://github.com/jingguo-math/gCQrK>, 2025.
- [14] J. Guo and M. Lopez-Fernandez. Generalized convolution quadrature for non smooth sectorial problems. *Calcolo*, 62(1):1–37, 2025.
- [15] E. Hairer and G. Wanner. *Solving Ordinary Differential Equations II, Second Revised Edition*. Springer-Verlag, Berlin, Heidelberg, 2010.
- [16] B. Jin, B. Li, and Z. Zhou. Correction of high-order BDF convolution quadrature for fractional evolution equations. *SIAM J. Sci. Comput.*, 39(6):A3129–A3152, 2017.
- [17] B. Li and S. Ma. Exponential convolution quadrature for nonlinear subdiffusion equations with nonsmooth initial data. *SIAM J. Numer. Anal.*, 60(2):503–528, 2022.
- [18] J.-R. Li. A fast time stepping method for evaluating fractional integrals. *SIAM J. Sci. Comput.*, 31(6):4696–4714, 2009/10.
- [19] M. López-Fernández. *Discretizaciones de orden espectral de integrales de contorno sectoriales y aplicaciones a problemas de evolución*. PhD thesis, Universidad de Valladolid, 2005.
- [20] M. López-Fernández, C. Lubich, C. Palencia, and A. Schädle. Fast Runge-Kutta approximation of inhomogeneous parabolic equations. *Numer. Math.*, 102(2):277–291, 2005.
- [21] M. Lopez-Fernandez and S. Sauter. Generalized convolution quadrature with variable time stepping. *IMA J. Numer. Anal.*, 33(4):1156–1175, 2013.
- [22] M. Lopez-Fernandez and S. Sauter. Generalized convolution quadrature with variable time stepping. Part II: Algorithm and numerical results. *Appl. Numer. Math.*, 94:88–105, 2015.
- [23] M. Lopez-Fernandez and S. Sauter. Generalized convolution quadrature based on Runge-Kutta methods. *Numer. Math.*, 133(4):743–779, 2016.
- [24] C. Lubich. Discretized fractional calculus. *SIAM J. Math. Anal.*, 17(3):704–719, 1986.
- [25] C. Lubich. Convolution quadrature and discretized operational calculus. I. *Numer. Math.*, 52(2):129–145, 1988.
- [26] C. Lubich. Convolution quadrature and discretized operational calculus. II. *Numer. Math.*, 52(4):413–425, 1988.
- [27] C. Lubich. On the multistep time discretization of linear initial-boundary value problems and their boundary integral equations. *Numer. Math.*, 67(3):365–389, 1994.
- [28] C. Lubich. Convolution quadrature revisited. *BIT*, 44(3):503–514, 2004.
- [29] C. Lubich and A. Ostermann. Runge-Kutta methods for parabolic equations and convolution quadrature. *Math. Comp.*, 60(201):105–131, 1993.
- [30] C. Lubich and A. Schädle. Fast convolution for nonreflecting boundary conditions. *SIAM J. Sci. Comput.*, 24(1):161–182, 2002.
- [31] W. McLean, I. H. Sloan, and V. Thomée. Time discretization via Laplace transformation of an integro-differential equation of parabolic type. *Numer. Math.*, 102(3):497–522, 2006.

- [32] I. Podlubny. *Fractional differential equations*, volume 198 of *Mathematics in Science and Engineering*. Academic Press, Inc., San Diego, CA, 1999. An introduction to fractional derivatives, fractional differential equations, to methods of their solution and some of their applications.
- [33] S. G. Samko, A. A. Kilbas, and O. I. Marichev. *Fractional integrals and derivatives: theory and applications*. CRC Press, Basel, 1993.
- [34] S. A. Sauter and C. Schwab. Boundary element methods. In *Boundary Element Methods*, pages 183–287. Springer, 2010.
- [35] L. Zhu, L. Ju, and W. Zhao. Fast high-order compact exponential time differencing Runge–Kutta methods for second-order semilinear parabolic equations. *J. Sci. Comput.*, 67:1043–1065, 2016.